Sheath Boundary Effects on the Stability of Hall Plasmas

A Thesis Submitted to the
College of Graduate and Postdoctoral Studies
in Partial Fulfillment of the Requirements
for the degree of Master of Science
in the Department of Physics and Engineering Physics
University of Saskatchewan
Saskatoon

By
Vincent Morin

Permission to Use

In presenting this thesis in partial fulfilment of the requirements for a Postgraduate degree from the University of Saskatchewan, I agree that the Libraries of this University may make it freely available for inspection. I further agree that permission for copying of this thesis in any manner, in whole or in part, for scholarly purposes may be granted by the professor or professors who supervised my thesis work or, in their absence, by the Head of the Department or the Dean of the College in which my thesis work was done. It is understood that any copying or publication or use of this thesis or parts thereof for financial gain shall not be allowed without my written permission. It is also understood that due recognition shall be given to me and to the University of Saskatchewan in any scholarly use which may be made of any material in my thesis.

Requests for permission to copy or to make other use of material in this thesis in whole or part should be addressed to:

Head of the Department of Physics and Engineering Physics
University of Saskatchewan
163 Physics Building, 116 Science Place
Saskatoon, Saskatchewan S7N 5E2
Canada

Or

Dean
College of Graduate and Postdoctoral Studies
University of Saskatchewan
116 Thorvaldson Building, 110 Science Place
Saskatoon, Saskatchewan S7N 5C9
Canada

Abstract

Plasma devices based on the $\mathbf{E} \times \mathbf{B}$-field configuration (where the externally applied electric and magnetic fields are everywhere perpendicular) are used for a variety of applications such as electric propulsion (i.e., Hall thrusters), diagnostic tools (e.g., Penning trap) and plasma processing of materials (i.e., magnetrons). Transverse electron current due to the electric and magnetic forces as well as diamagnetic flows due to the presence of pressure and magnetic field gradients are the sources of gradient-drift instabilities which result in turbulence and anomalous transport (the transport of particles, momentum and energy that cannot be explained by theory). Most investigations into plasma instabilities for various configurations of the fields and plasma parameters have been done under the assumption that the plasma is unbounded and, therefore, in neglect of any boundary effect. However, the presence of physical boundaries may significantly alter the dynamics of the plasma by restricting the parallel electron dynamics and introducing plasma sheath regions (regions where quasi-neutrality is violated) near the walls. Previous works have shown that conservation of charge at the boundary of the plasma affects the instability criteria for the gradient-drift modes as well as result in new instabilities. Effects of the sheath boundary conditions on the instabilities of partially magnetized plasmas are further investigated in this project. It is shown, for the first time, that sheath dissipation results in the instability of the anti-drift mode (i.e. the Simon-Hoh instability) due to the plasma density gradient. It is also shown that sheath dissipation results in a strong instability in conditions where the criterion for the standard Simon-Hoh instability (which results from the difference in electron and ion drifts together with a density gradient) is not satisfied; this result is important as it may provide an explanation for anomalous transport when the Simon-Hoh instability is absent. Then, including the electric potential induced by the sheath as well as the sheath boundary condition, one arrives at a set of two nonlinear ordinary differential equations with a non-local integral condition. The boundary conditions are finally derived consistent with the sheath to fully define the boundary-value problem.

Acknowledgements

I would like to take this opportunity to thank all of those who were instrumental to my academic success. First and foremost, I would like to thank my supervisor, professor Andrei Smolyakov, for his support, helpful criticism and enlightening guidance. I would also like to thank professor Chijin Xiao without whom I wouldn't have had the chance to come to the University of Saskatchewan to pursue a Master's degree in Physics.

I would be remiss if I did not acknowledge the contribution of Dr. Oleksandr Koshkarov to this research project. Since my arrival in the theoretical plasma group, he played the role of mentor and helped me on numerous occasions. My thanks also extend to all my colleagues who provided valuable feedback and insightful discussions through the past two years. Thank you also to the Natural Sciences and Engineering Research Council and the University of Saskatchewan for providing me with financial support and enabling me to concentrate on my research project.

Of course, I would like to thank all my family and friends who provided me with support and encouragements through good and challenging times.

A special thank you to my beautiful wife Emilia for supporting me throughout the years. Thank you for your patience through the long work hours and your never ending love.

I would like to dedicate this thesis to my beloved wife Emilia

Contents

Permission to Use i

Abstract ii

Acknowledgements iii

Dedication iv

Contents v

List of Tables vii

List of Figures viii

Chapter 1: Introduction 1
- 1.1 Plasma Devices . . . 2
- 1.2 Motivation . . . 3
- 1.3 Thesis Breakdown . . . 4

Chapter 2: Plasma Sheath Theory 6
- 2.1 Dynamical Formation of the Sheath . . . 8
- 2.2 Early Days of Langmuir, Harrisson & Thompson . . . 13
- 2.3 Numerical & Fluid Solutions . . . 18
- 2.4 The State of Plasma Sheath Theory Today . . . 21

Chapter 3: Classical Instabilities in Cold Plasmas 24
- 3.1 Fluid Equations . . . 25
- 3.2 Simon-Hoh Instability . . . 28
- 3.3 Resistive Instability . . . 30

Chapter 4: Modification of the Simon-Hoh Instability by Sheath Effects in Partially Magnetized Hall Plasmas 32
- 4.1 Introduction . . . 32
- 4.2 Governing Equations . . . 35
- 4.3 Results & Analysis . . . 36
- 4.4 Summary . . . 41

Chapter 5: Boundary Value Problem for a Perturbed Hall Plasma with Sheath Effects 45
- 5.1 Introduction . . . 45
- 5.2 Basic Equations . . . 47
- 5.3 Sheath Boundary Condition . . . 51

5.4 Summary 54

Chapter 6: Conclusion **55**

References **57**

Appendix A: Mathematica Code **60**

Appendix B: Detailed Calculations **69**
B.1 Full Solution to the Dispersion Equation 69
B.2 Instability when the standard Simon-Hoh instability is not operative 70
B.3 Equation B.2 to 1st-Order in $\nu_{\|}$ 71
B.4 Equation B.2 to 2nd-Order in $\nu_{\|}$: Near the Simon-Hoh Transition to Instability 72
B.5 Equation B.2 for Vanishing Perpendicular Wave-Number 72
B.6 Perturbed Electron Flux $\tilde{\mathbf{\Gamma}}_e$ 73

Appendix C: Mathematical Identities **74**
C.1 Schlömilch's Transformation 74
C.2 Fractional Calculus 74

List of Tables

4.1 Penning discharge and magnetrons parameters in different regimes. The plasma length along the magnetic field in Ref [1] ($L = 0.4$ cm) is an estimate and we have estimated that $\nu_{en} \sim 10^6$ Hz for the electron-neutrals collision frequency [2]. 44

B.1 θ for the different signs of a and b 70

List of Figures

1.1 Hall plasma device and field configuration (used in this project) [3]. 2
1.2 Field configuration for a Penning Trap [4] and Magnetron [5]. The cathode of the magnetron is not shown on the diagram since only the target (anode) is shown; the cathode is typically the source of ions for implantation which would be, in this picture, above the target. 3

2.1 Coordinate system for the growing sheath [6]. 9
2.2 Approximate form of the electric potential $-e\phi/T_e = z^2/2L^2$ that satisfies Eq. 2.18 assumed in this project versus the exact solution as well as the fluid solution given in the next section (see Eq. 2.32). 18
2.3 Normalized electric potential versus normalized position [7]. Here, the ionization is proportional to the electron density, so that the sheath position $s_0 = 0.405$ instead of $s_0 = 0.344$. 20

4.1 The collisionless Simon-Hoh instability and its modification due to the sheath resistivity with $\nu_\parallel/\omega_{ci} = 0.01$ and $k_y\rho_s = 1$ when the threshold for the instability disappears [2]. It should be mentioned that the normalization constant used here, the ion cyclotron frequency ω_{ci}, is used since it is related to the electron cyclotron frequency (an important frequency constant of a Hall plasma) and the proportionality constant $(\sqrt{m_e/m_i})$ is more convenient for the representation of the results. 39
4.2 The real and imaginary part of the mode frequency as a function of $\nu_\parallel/\omega_{ci}$ for $v_0 = 0$. The maximum value of the growth rate, $\gamma \approx 0.322\omega_{ci}$, occurs at $\nu_\parallel \sim \omega_*/2$. For $\nu_\parallel \to 0$, $\omega \to k_\perp^2 c_s^2/\omega_*^2$, and for $\nu_\parallel \to \infty$, $\omega = k_y c_s$ [2]. 40
4.3 ω/ω_{ci} as a function of $\nu_\parallel/\omega_{ci}$ for $k_y\rho_s = 1$ and vanishing v_*. In the opposite limit of $\nu_\parallel \to \infty$, one finds $\omega = \omega_{ci}$ as expected. The maximum value of the growth rate, $\gamma \approx \omega_0/3$, occurs at $\nu/\omega_{ci} \approx c_s/v_0$. In the limit of vanishing $\nu_\parallel \to 0$, $\omega = \omega_0$ [2]. 41
4.4 γ/ω_{ci} as a function of $\nu_\parallel/\omega_{ci}$ for $k_y\rho_s = 1$ and $\omega_*/\omega_{ci} \sim 7$. The maximum of the growth rate increases with ω_0 [2]. 42
4.5 ω_r/ω_{ci} as a function of $\nu_\parallel/\omega_{ci}$ for $k_y\rho_s = 1$ [2]. 42
4.6 ω_r/ω_{ci} as a function of (small) $\nu_\parallel/\omega_{ci}$ for $k_y\rho_s = 1$ [2]. 43
4.7 ω/ω_{ci} as a function of $\nu_\parallel/\omega_{ci}$ [2]. 43

Chapter 1

Introduction

Plasmas are by far the most common state of (regular) matter found in the universe; of all the visible matter, 99.9% is in the form of an ionized gas. It is often referred to as the fourth state of matter and may be reached by heating a gas to the extent that the kinetic energy of the bound electrons exceeds its electrical binding energy to the atoms of the gas, thus creating a substance made of ions and electrons in an equilibrium state. Typical temperatures in laboratory plasmas are of the order of $10\ eV \sim 116\,000\ K$, but space plasmas may have temperatures as low as $100\ K$. Plasma density may range over several orders of magnitude from very low density plasmas, such as auroras, to very high density plasmas such as the one found in the imploding deuterium-tritium pallets in inertial fusion devices.

Since plasmas are collections of charged particles and the Coulomb force is long-range, they exhibit collective dynamics seldom found in neutral fluids. This makes plasmas extremely more intricate and allows for a very large set of collective oscillation modes interacting with each other as well as with the electromagnetic fields present. Given the great number of physical phenomena present in a plasma at any given set of parameters, it is the job of the plasma physicist to determine the right assumptions to factor out all unnecessary complications to study the behaviour of a given plasma and the important phenomena that may emerge (in particular, any instability that may arise from small perturbations). This is not a trivial task, but many decades of research in this area as provided this field with several approaches (fluid, kinetic, gyrokinetic, etc.) and key assumptions (cold ions, unmagnetized ions, isothermal electrons, etc.) that serve to effectively reduce the complexity of a problem and focus on the phenomena pertinent to it. In this project, much emphasis is set on the assumptions that the $\mathbf{E} \times \mathbf{B}$ plasmas under investigation have unmagnetized, cold ions (to avoid Landau damping) and warm, magnetized electrons; this means that the thermal energy

of ions is much smaller than their electrical potential energy while electrons have thermal energy of the order of their electrical potential energy and that the gyroradius of the ions, contrary to the electrons, is much larger than any length scale of the system. Thus, a two-fluid description of the plasma is used. This serves to study specific instabilities such as the Simon-Hoh and two-stream instabilities in detail.

1.1 Plasma Devices

Hall plasmas are a specific type of confined plasma in which the externally applied electric and magnetic fields are perpendicular (i.e. $\mathbf{E} \times \mathbf{B}$-field configuration) and the plasma is partially magnetized (i.e. it is assumed that the ions are unmagnetized while the electrons are fully magnetized).

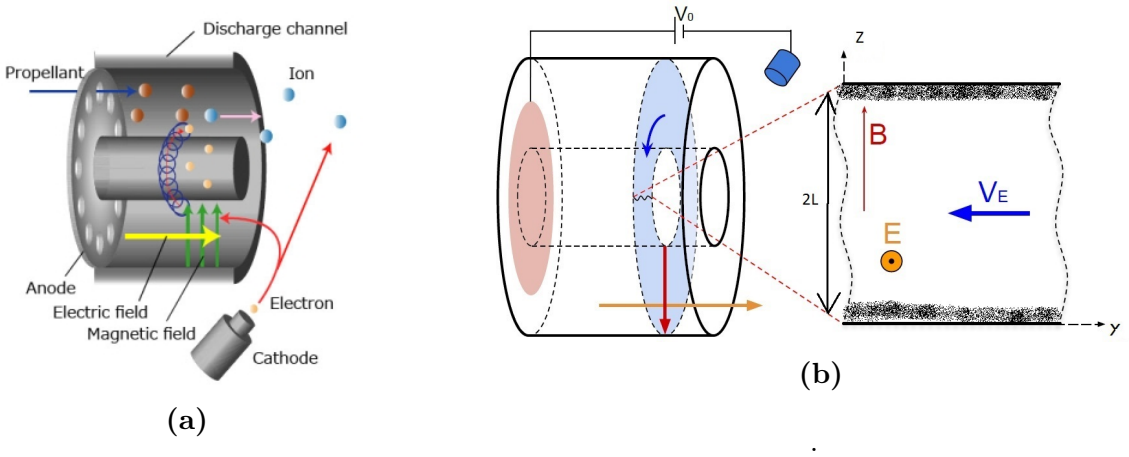

Figure 1.1: Hall plasma device and field configuration (used in this project) [3].

Many devices use this type of plasma. The first example is the Hall thruster from which the name for this type of plasma originates (Fig. 1.1b shows a typical cross-field configuration with appropriate axes that will be used in this thesis). As a second example, there is the Penning trap which is very similar to the Hall thruster, but involves a significantly weaker electric field as no ions need to be accelerated. The field configuration is similar in that the electric field and magnetic fields are perpendicular at the center of the device. Thirdly, there is the magnetron, a device used mostly for ion implantation.

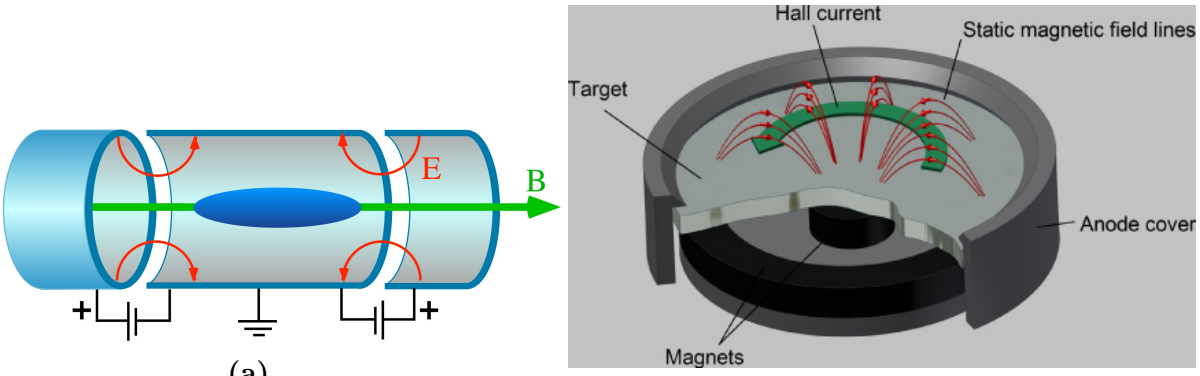

(a) (b)

Figure 1.2: Field configuration for a Penning Trap [4] and Magnetron [5]. The cathode of the magnetron is not shown on the diagram since only the target (anode) is shown; the cathode is typically the source of ions for implantation which would be, in this picture, above the target.

All these devices have the similar electric and magnetic fields configuration. Therefore, they may be analyzed using the same approach and must then also share the same instabilities, albeit their growth rates and eigen-frequencies may differ by several orders of magnitude depending on the strength of the parameters.

1.2 Motivation

This research project has the main goal of exploring the dynamics of Hall plasmas and similar $\mathbf{E} \times \mathbf{B}$-field configuration plasmas in the presence of sheaths. Since the system is finite along the magnetic field direction, one needs to take into account the dynamics of the electrons and ions at the boundaries. In a first approximation, one may assume that the perturbations satisfy $k_z^2 \ll k_y^2$ such that the sheaths only affect the currents reaching the walls. Going one step further, one may consider the full boundary-value problem that arises from having a plasma finite along the magnetic field line; then, with the right boundary conditions at the sheath edge, one may solve the problem for perturbations within the plasma. Any instability may then be found from the dispersion equation that arises from applying the boundary conditions to general solutions to the differential equation.

1.3 Thesis Breakdown

The thesis will be structured in the following manner. First, a chapter will be dedicated to introducing the reader to the plasma sheath. A description of the dynamics of the plasma leading to the formation of a stable sheath will be first given. Then, the steady-state of a plasma when sheaths are present will be presented with an emphasis on the early pioneers such as Langmuir, Tonks, Harrisson and Thompson and their contributions to the theory. The major advances in numerical solutions to the problem due to the advances of efficient computers will subsequently be presented as well as some results derived from a fluid description of the plasma.

The third chapter will explore two important instabilities present in partially magnetized $\mathbf{E} \times \mathbf{B}$ plasmas: the resistive instability (when a resistive term, such as electron-neutral collisions, is included) and the Simon-Hoh instability (when a density gradient parallel to the externally applied electric field exists). This chapter will serve as an introduction to the two instabilities that are relevant to bounded, Hall plasmas.

Chapter 4 will present what can be considered a first-order approximation to the presence of sheaths in bounded plasmas (i.e., assuming $k_z^2 \ll k_y^2$). This chapter will explore the effects of sheaths on the stability of the plasma and, more importantly, on the Simon-Hoh instability. It will be shown that near the transition to the unstable Simon-Hoh instability, the growth rate and oscillation frequency are significantly modified by the effect of the sheath which behaves as a collisional term. Consequently, an instability of the resistive type was found to exist when the Simon-Hoh instability was absent.

Finally, chapter 5 will investigate the problem of bounded plasmas without any assumption regarding the perturbation wavelength along the magnetic field. The appropriate boundary-value problem will be given as well as the boundary conditions consistent with the presence of the sheath. It will be also shown that, to be consistent with a static sheath, a net ion flow into the sheath region is necessary. In the previous chapter, the flow was neglected in the plasma and the ion speed was assumed to be equal to Bohm's velocity at the sheath edge. In this chapter, however, the net ion flow is included. Accordingly, the problem reduces to a set of two nonlocal, ordinary differential equations for the perturbed electric potential and

ion velocity. With the problem well-posed and the appropriate boundary conditions given, its solution will be left for future works as a numerical scheme needs to be determined.

The main idea behind this form of exposure to the problem of bounded plasmas and plasma-sheath interactions is to provide the reader with an understanding of the origin of the stable plasma sheath as well as the equations describing it and their limitations (i.e. assuming quasi-neutrality everywhere in the plasma) and how the boundary conditions used in this research project arise naturally from the formation and steady-state configuration of the sheath (i.e. the Bohm velocity condition on the ions entering the sheath and the shape of the electric potential within the plasma). Then, the system of equations and results derived for the bounded Hall plasma will seem to arise naturally from the considerations of a plasma with static sheaths at its boundaries.

Chapter 2

Plasma Sheath Theory

A plasma is a collection of charged particles in equilibrium. Therefore, their exist, on the scale of the mean distance between electrons and ions, complex electric and magnetic fields that permeate the plasma; a full description of the dynamics of each particle in the plasma is very difficult, although some modern super-computers may be up to the task. However, it is possible to describe the plasma as a continuous, electrically neutral fluid if the phenomena one is interested in occur over length scales larger than a specific length; the Debye length. Simply put, every charged particles in the plasma repel like charges and attract opposite charges; then, in a region near a given charge, there will be slightly more charges of the opposite sign that will effectively screen that charge from any particle outside that region.

Consider a sphere of radius λ_D around an electron which was explored in Ref. [8]. Then, Poisson's equation gives us, upon inserting an electron in a quasi-neutral plasma,

$$-\frac{1}{r^2}\frac{d}{dr}\left(r^2\frac{d\phi}{dr}\right) = 4\pi e(n_i(r) - n_e(r) - \delta^{(3)}(\mathbf{r})), \tag{2.1}$$

where ϕ is the electric potential, $n_{i,e}$ are the ion and electron densities in the quasi-neutral plasma and e is the electric charge of an electron. Assuming the ions are motionless (since the electrons are so much lighter and thus react to the inserted charge more readily) and electrons are originally in thermal equilibrium, the electron density is given by $n_e(r) = n_0 e^{e\phi(r)/T_e}$. Assuming further that $e\phi/T_e \ll 1$, Eq. 2.1 becomes,

$$\frac{1}{r^2}\frac{d}{dr}\left(r^2\frac{d}{dr}\frac{e\phi(r)}{T_e}\right) - \frac{1}{\lambda_D^2}\frac{e\phi(r)}{T_e} = \frac{4\pi e^2}{T_e}\delta^{(3)}(\mathbf{r}), \tag{2.2}$$

where $\lambda_D^2 = T_e/4\pi n_0 e^2$ is called the Debye length. This has the form of the screened Poisson equation. Therefore, transforming to Fourier space, solving for the electric potential and then

transforming back to normal space, the solution reduces to $\phi(r) = (-e/r)e^{-r/\lambda_D}$. Hence, over distances of the order of the Debye length, the electric potential due to a single charge falls off exponentially.

When a conducting or dielectric wall is introduced in a plasma, similar dynamics lead to the creation of the sheath region previously mentioned. Since electrons are much lighter than ions, they are free to escape the plasma through the bounding walls much more quickly than the ions which are impaired by their inertia. For a floating or dielectric wall, these electrons create a surface charge that further attracts the ions and repels the electrons from leaving the plasma through the wall. A steady-state is then reached forming what is called a sheath at the plasma-wall interface and spanning several Debye lengths into the plasma; this phenomenon was first explained theoretically by Irving Langmuir in 1923 [9]. Hence, no electric field due to the wall can penetrate the plasma further than the sheath region. However, as will be seen in the next section, the formation of a stable ion sheath leaves a footprint in the plasma: a net ion drift which creates a small, but not negligible, electric field that permeates the bulk plasma and that vanishes only at the center (due to the symmetry of the problem).

The sheath has been the subject of much research and speculation over the past several decades. To this day, we do not have an analytical solution for the different plasma parameters (ion and electron number densities, electric potential, etc.) that satisfies both the bulk plasma where quasi-neutrality applies and the plasma sheath where space-charge is significant and equilibrium is reached due to ion flow. This is due mostly to the difficulty in solving the integro-differential equation that emerges from the kinetic description of the plasma and the use of Poisson's equation from electromagnetic theory. However, much work as been done both analytically and numerically though the past several decades.

This chapter introduces, first, the dynamical formation of the sheath and, second, the history behind the analytical and numerical descriptions of the steady state plasma sheath. Understanding this region of the plasma is crucial to understanding the boundary conditions to be imposed on any confined plasmas and the resulting effects on instabilities within them.

2.1 Dynamical Formation of the Sheath

Up to the 1970s, much of the work done on the sheath problem assumed the existence and stability of the sheath (these works will be reviewed in the next sections). It was taken for granted that a steady-state was reached in all plasmas subjected to the introduction of a metal or dielectric boundary and the existence of a source of ions within the bulk plasma. Further, Bohm's condition seemed to be, at least for a quasi-neutral plasma, taken for granted and the ions were assumed to be accelerated in some manner to the Bohm velocity; very little explanation was given for the specific dynamics of the ions at the moment of creation of the sheath and its stabilization. However, borrowing from neutral fluid dynamics, several qualitative arguments may be made regarding the state of the plasma as the sheath grows into it.

Any perturbation (induced, for example, by the introduction of an electrode in the plasma) will propagate as a wavefront with a specific velocity into the plasma. Physically, the problem is equivalent to that of a pressurized container whose bounding surface is suddenly removed (e.g., a balloon). Classical theory of fluid dynamics tells us that an expansion wave will propagate inside the fluid volume at the local speed of sound to induce motion in the fluid in order to achieve thermal and mechanical equilibrium with the new boundary surface (e.g. the fluid that surrounds the balloon rather than the previous balloon surface). In our case, the new boundary condition is the presence of a surface charge density due to the electrons that were captured by the wall. This new distribution of electrons is not an equilibrium state of the plasma when the ions are distributed uniformly. Then, the transition to a new equilibrium state is achieved by the propagation of a disturbance into the plasma at the local (modified) speed of sound of the ions, $c_s = \sqrt{T_e/m_i}$, termed Bohm's velocity. The question, however, remains what the sheath exactly represents and its relation to the new ion and electron equilibrium state.

From 1970 to 1973, several important works [6, 10, 11, 12] on the subject of sheath formation and stability laid the theoretical foundation following the experimental work of Chester [13]. The main idea used in these publications was to consider the plasma, at the instance of insertion of an electrode into the plasma, as being a cold ion fluid with the

electrons being free to move in order to respond to the new boundary condition. Then, they will distribute themselves isothermally along the magnetic field lines (i.e., $n_e = n_0 e^{e\phi/T_e}$) perpendicularly to the wall. The sheath then starts to form as the ions react to the new distribution of electrons, being attracted towards the now negatively charged electrode. Here, I will follow Refs. [6, 12, 14]. The following derivation of the sheath position as a function of time will serve to explain the formation of the sheath as well as explain the origin of the ion dynamics at steady state (i.e., the creation of a rarefaction wave and Bohm's condition).

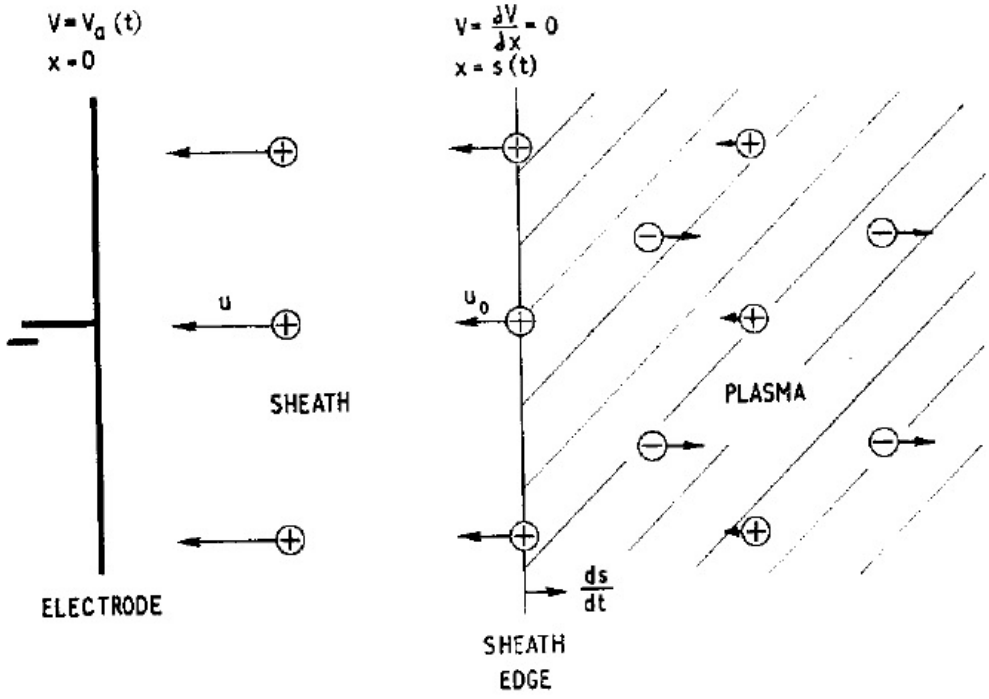

Figure 2.1: Coordinate system for the growing sheath [6].

Following Andrews and Varey [6], the main assumptions are that the electrons respond instantaneously, the ions are monoenergetic, there is no reflection or secondary emission of ions at the electrode, the plasma is collisionless in the sheath, there are no electrons in the sheath and the electric field vanishes at the sheath boundary (a good approximation as the electric field in the presheath is much smaller than the electric field in the sheath). Then, looking at the ion equations of motion and continuity in the sheath as well as Poisson's equation, one finds, taking the electrode as the origin of our coordinate system as shown in Fig. 2.1,

$$-\frac{\partial^2\phi}{\partial x^2} = 4\pi e n_i, \tag{2.3}$$

$$\frac{\partial v_i}{\partial t} + \frac{\partial}{\partial x}\left(\frac{1}{2}v_i^2 + \frac{e}{m_i}\phi\right) = 0, \tag{2.4}$$

$$\frac{\partial n_i}{\partial t} + \frac{\partial}{\partial x}(n_i v_i) = 0, \tag{2.5}$$

with the boundary conditions at the sheath edge ($x = s$), $\phi = \partial\phi/\partial x = 0$ (we are free to choose the origin of the electric potential to be at the sheath edge). Assuming the sheath moves at constant velocity, one can use a Galilean transformation (transformation between inertial frames that preserves the laws of motion) to go to the frame of reference of the moving sheath edge and the dependent variables become $t' = t$ and $x' = x - (ds/dt)t$ where ds/dt is the constant speed of propagation. Then, the set of equations 2.3 , 2.4 and 2.5 become, in the new frame of reference,

$$-\frac{\partial^2\phi}{\partial x'^2} = 4\pi e n_i, \tag{2.6}$$

$$\frac{\partial v_i'}{\partial t'} + \frac{\partial}{\partial x'}\left(\frac{1}{2}v_i'^2 + \frac{e}{m_i}\phi\right) = 0, \tag{2.7}$$

$$\frac{\partial n_i}{\partial t'} + \frac{\partial}{\partial x'}(n_i v_i') = 0, \tag{2.8}$$

For steady-state in the lab frame of reference, the terms $\partial v_i'/\partial t'$, $\partial n_i/\partial t'$ in the sheath frame must vanish (to maintain Galilean invariance) and the sheath moves with constant velocity so that the acceleration term, $\partial^2 s/\partial t'^2$, vanishes. Then, this set of equations is equivalent to the Child-Langmuir problem with the boundary condition of finite ion velocity into the sheath; this velocity is necessary to conserve charge within the sheath. The solution for the sheath potential is then given, using the conservation of mass and momentum of the ions in the sheath, by the differential equation for the electric potential,

$$\frac{\partial^2\phi}{\partial x'^2} = -4\pi n_0 e\left(1 - \frac{2e\phi}{m v_0'^2}\right)^{-1/2}, \tag{2.9}$$

where $v_0' = v_0 - ds/dt$ is the ion velocity entering the sheath in the sheath frame of reference. For a static sheath to exist (i.e. $ds/dt = 0$, the sheath is at rest in the lab frame), the ion

velocity entering the sheath in the lab frame v_0 must be finite such that the v_0' be nonzero; otherwise, no solution for the electric potential in the sheath region would be possible. The integration should now be taken from the sheath edge towards the electrode; in other words, from $x' = 0$ to some point x'. Further, since we assume the electric potential is strictly decreasing from 0 at the sheath edge, any value is negative within the sheath. The result is,

$$(s-x)^2 = \frac{4}{9}\frac{m(v_0 - ds/dt)^2}{8\pi n_0 e^2}\left[\left(1 + \frac{2e\phi}{m(v_0 - ds/dt)^2}\right)^{3/2} + 3\frac{2e\phi}{m(v_0 - ds/dt)^2} - 1\right]. \quad (2.10)$$

Assuming the electric potential drop is very large, we recover Child's law,

$$\frac{(s-x)^2}{\lambda_D^2} = \frac{4\sqrt{2}}{9}\frac{c_s}{|v_0 - ds/dt|}\left(\frac{e\phi}{T_e}\right)^{3/2} \quad (2.11)$$

At the moment of formation, the sheath grows very fast and the ions in front of the sheath edge are still in a static state; then, $ds/dt \gg v_0$. Then, for a finite system, steady-state is reached when the sheath's growth stops; then, $ds/dt \ll v_0$. At this point, it will be taken as given that the velocity $v_0 = c_s = \sqrt{T_e/m_i}$, Bohm's velocity; a full derivation of this will be given in the next section as it involves specific assumptions about the plasma bulk. However, one way of motivating this is to consider the ions as freely "falling" into the sheath due to the small, but not negligible, electric field in the presheath. Since the sheath edge represents, in the quasi-neutral approximation, a surface of discontinuity in the plasma, it is reasonable to assume the ions reach at that point the local (modified) speed of sound (i.e. Bohm's velocity) similarly to a gas expanding into a vacuum. Then, at steady-state, the ions entering the sheath do so with Bohm's velocity.

To explain the origin of the rarefaction wave necessary to accelerate the ions to c_s, it is best to follow the work of Murakami [14]. Assuming, for simplicity, that at any given time Child's law applies, then, as will be seen below, the sheath expands, at first, supersonically until the sheath thickness reaches a factor of $e^{-1/2} \approx 0.6$ of its steady-state size and then expands subsonically creating a rarefaction wave.

In the first instances of the inclusion of a material wall into the plasma, the electrons are attracted and quickly escape the plasma leaving a small region near the wall mostly positive as the ions, due to their large inertia, have not yet responded to the presence of the wall.

Then, as their move towards the wall, their motion is impeded by space-charge. The ions thus reach, in the rest frame of the sheath edge, the limiting outgoing flux provided by the Child-Langmuir law seen previously,

$$s^2 = \frac{4}{9}\frac{2e/m}{n_0 e|v_0 - ds/dt|}(-\phi_w)^{3/2}, \tag{2.12}$$

where $\phi_w < 0$ is the wall potential relative to the plasma potential and s is the sheath thickness. Since the sheath expands initially supersonically, the ions are still motionless and the incoming ion flux is given by $\Gamma_i = n_0 ds/dt \gg n_0 v_0$. Then, neglecting the v_0 term in Eq. 2.12 and solving of the sheath velocity ds/dt, one finds

$$n_0 m\frac{ds}{dt} = \frac{8}{9}\frac{1}{s^2}(-\phi_w)^{3/2}. \tag{2.13}$$

As expected, the sheath velocity decreases with increasing sheath thickness s; then, the transition to subsonic speed, $ds/dt < c_s$, is inevitable. At that moment, a rarefaction wave is created, moving with Bohm's velocity. The rarefaction wave then propagates in front of the sheath accelerating the ions such that the velocity of the ions entering the sheath region satisfy $|v_0 - ds/dt| = c_s$. Therefore, as the sheath velocity, ds/dt, decreases lower than c_s, the ion velocity, v_0, in the lab frame must increase. As the sheath velocity goes to zero, Eq. 2.12 converges to a specific value for the sheath thickness as a function of the electron temperature, electron and ion masses as well as the number density within the bulk plasma (the equilibrium electric potential at the wall being a function of these same parameters [15]).

It should now be clear to the reader that the creation of the sheath as well as reaching steady-state necessitates a net ion flow from the plasma into the sheath region and a source of ions within the plasma. For simplicity, one usually assumes a uniform and steady rate of ion generation; this will be assumed in subsequent sections. Up to this point, any net electric field within the plasma was neglected; this is, of course, not true as some small electric field is necessary to accelerate the ions from rest (at the center of the plasma) to Bohm's velocity at the sheath edge. The next section will provide a quantitative derivation of the electric potential distribution within the plasma at steady-state as well as demonstrate how Bohm's condition comes about.

2.2 Early Days of Langmuir, Harrisson & Thompson

In 1959, E.R. Harrison and W.B. Thompson published a paper that provided the first analytical solution to the problem of the planar plasma sheath [16]. Langmuir had already solved the problem using a series approximation, but Harrison and Thompson used the Schlömilch's transformation to solve the integral equation for the unknown electric potential exactly. In doing so, they found an analytical expression relating the electric potential to the electric field at any point within the bulk plasma up to the plasma sheath interface. Because they were assuming quasi-neutrality within the plasma, the sheath interface was well-defined as the location where the electric field diverges to infinity. The authors used this to calculate both the electric potential and position of the plasma sheath; the result agreed perfectly with the numerical values tabulated a few decades earlier by Langmuir.

Consider the Vlasov equation for the distribution function of the ions in the plasma herein assumed to be planar, finite in the z-direction and infinite in all other directions. Let the z-axis extend from the center of the plasma to the edge of the sheath. Then, at steady-state, with the ion source term per unit volume $g(z)$ and the assumption that the ions are created at rest in the plasma through ionization,

$$v\frac{\partial f}{\partial z} + \frac{F}{m}\frac{\partial f}{\partial v} = g(z)\delta(v). \tag{2.14}$$

In the range $z \in [\epsilon, \epsilon + d\epsilon]$, the ion number density must satisfy the continuity equation,

$$vf(\epsilon, v)dv = g(\epsilon)d\epsilon. \tag{2.15}$$

Since the ions arriving at ϵ from any point z within the plasma are accelerated by the local electric field, one has, using conservation of energy,

$$v(\epsilon) = \sqrt{\frac{2e(\phi(\epsilon) - \phi(z))}{m_i}}. \tag{2.16}$$

Then, using quasi-neutrality and the assumption that the electrons are distributed isothermally,

$$n_0 e^{e\phi(z)/T_e} = \frac{1}{\sqrt{2}c_s}\int_0^z \frac{g(\epsilon)}{\sqrt{e\phi(\epsilon)/T_e - e\phi(z)/T_e}}d\epsilon, \tag{2.17}$$

where $c_s = \sqrt{T_e/m_i}$. Eq. 2.17 may be solved either, as Langmuir, as a series solution or, following Harrison and Thompson, by using the Schlömilch's transformation. From the latter method (described in Appendix D) whilst taking $\eta(z) = -e\phi(z)/T_e = x^2$ and $\eta(\epsilon) = -e\phi(\epsilon)/T_e = x^2 sin^2\theta$, one finds the exact solution,

$$\frac{\pi}{\sqrt{2}}g(\eta)\sqrt{\eta}\frac{dz}{d\eta} = c_s n_0 \left(1 - 2\sqrt{\eta}D(\sqrt{\eta})\right), \tag{2.18}$$

where $D(x) = e^{-x^2}\int_0^x e^{t^2}dt$ is the Dawson function [1]. Clearly, for a specific value for the normalized electric potential η_* such that $1 - 2\sqrt{\eta_*}D(\sqrt{\eta_*}) = 0$ the electric field becomes infinite; hence, one may use this to define the plasma-sheath edge in the case of a quasi-neutral plasma (since we have neglected the space-charge term in Eq. 2.17). Using this definition, the plasma-sheath edge becomes the position at which quasi-neutrality fails. The value can be found numerically using tabulated values of the Dawson function, the result being $\eta_* = 0.8539$ and the position of the sheath is found by integrating Eq. 2.18. For a uniform rate of ion generation $g(z) = n_0\lambda$ in the bulk plasma, one finds $\lambda z/\sqrt{2}c_s = 0.344$. Therefore, it is clear that the sheath position is only a function of the ion mass, electron temperature and ion generation rate.

It is interesting to note that a more straightforward derivation is possible through the use of fractional derivatives (described in Appendix D). The trick is to recognize that Eq. 2.17 has the functional form of the half-integral of the source function $g(\eta(z))/\eta(z)'$; in other words, that equation may be recast as

[1] It should be noted that in their original paper [16], Harrison and Thompson used an old definition of the Dawson function which is now given, up to a constant, by the error function; the definition used in this thesis is consistent with the now accepted definition of the Dawson function is most mathematical resources

$$n_0 e^{-\eta} = \sqrt{\frac{\pi m_i}{2\kappa T_e}} \frac{d^{-1/2}}{d\eta^{-1/2}} \left(\frac{g(\eta(z))}{\eta(z)'} \right), \tag{2.19}$$

$$n_0 \frac{d^{1/2}}{d\eta^{1/2}} e^{-\eta} = \sqrt{\frac{\pi m_i}{2\kappa T_e}} \left(\frac{g(\eta(z))}{\eta(z)'} \right), \tag{2.20}$$

$$\frac{n_0}{\sqrt{\pi\eta}} \left(1 - 2\sqrt{\eta} D(\sqrt{\eta})\right) = \sqrt{\frac{\pi m_i}{2\kappa T_e}} \left(\frac{g(\eta(z))}{\eta(z)'} \right), \tag{2.21}$$

where it is assumed that all functions involved are differintegrable (i.e., they can be written in the form a generalized power series in x, $x^p \sum_{j=0}^{\infty} a_j x^j$ where p is any real number [17]); the exact definition of the fractional derivative may be found in Appendix C.2. The advantage of this derivation, other than being much more succinct and clear than that given in Harrison and Thompson's article [16], is that it enables the introduction in a more straightforward way of the space-charge term which becomes important near the sheath region. The differential equation would then be given as,

$$\lambda_D^2 \frac{d^{1/2}}{d\eta^{1/2}} \left(\frac{z''}{(z')^3} \right) - \frac{1}{n_0} z' \sqrt{\frac{\pi m_i}{2\kappa T_e}} g(\eta) + \frac{1}{\sqrt{\pi\eta}} \left(1 - 2\sqrt{\eta} D(\sqrt{\eta})\right) = 0, \tag{2.22}$$

where $z' = dz/d\eta$ and one needs to solve for $z(\eta)$ which is clearly highly non-trivial. The first term removes the singularity at η_* since, at the location η_*, the Poisson term becomes of the same order of magnitude as the other terms in Eq. 2.22 and may not be neglected. Now, because we have the semi-derivative of a product, one finds that the differential equation involves an infinite series of higher derivatives. This is outside the scope of this thesis as we will assume quasi-neutral plasma bulk.

When one assumes a quasi-neutral plasma, the plasma-sheath boundary is well-defined and the potential at this location does not depend on the potential of the wall (other then it being more negative since we assume strictly decreasing electric potential). If one assumes, in the simplest case, a uniform generation rate, then $g(\eta) = \lambda n_0$ (λ having the units of inverse seconds) and one finds,

$$z = \frac{\sqrt{2} c_s}{\lambda} \frac{2}{\pi} D(\sqrt{\eta}). \tag{2.23}$$

Hence, $z_* = 0.405\sqrt{2} c_s/\lambda$ measured from the center of the plasma. One can now define clearly the different regions: the plasma is the region where quasi-neutrality applies and the

sheath is the region that starts at z_* where space-charge cannot be neglected. The pre-sheath is a sub-region of the plasma and does not have a clear boundary within it; it does, however, have an end boundary, the sheath edge. The pre-sheath is ill-defined because it is defined as the region within the plasma where the electric field is non-zero. Unfortunately, as will be seen below, the electric field changes continuously from the center of the plasma until the edge of the sheath. Therefore, for the purpose of this thesis, we will restrict the use of the pre-sheath concept and simply refer to the region before the sheath as the plasma.

The ion flow rate into the sheath is

$$\Gamma_i = \int_0^{z_*} g(z)dz = \int_0^{\eta_*} \frac{\sqrt{2}n_0 c_s}{\pi}\left(\frac{1}{\sqrt{\eta}} - 2D(\sqrt{\eta})\right)d\eta = \frac{2\sqrt{2}}{\pi}n_0 c_s D(\sqrt{\eta_*}) \approx 1.144 n_0 c_s, \tag{2.24}$$

where the identity for the Dawson function ($D(x)' = 1 - 2xD(x)$) was used. It is interesting to notice that the (average) ion velocity at the sheath edge is slightly greater than Bohm's velocity and, therefore, Bohm's condition is satisfied; for the purpose of this thesis, the ion current density will be taken as en_0c_s exactly since only an approximation for the electric potential within the plasma will be used.

If one assumes that $e\phi(z)/T_e \ll 1$ for all $z < z_*$, then it is useful to expand the Dawson function in a series and invert it to recover an approximate solution for the electric potential as a function of z. The result is, up-to $\mathcal{O}(e\phi/T_e)^3$, given by,

$$C\frac{e\phi(z)}{T_e} = \frac{\pi^2}{8}\frac{\lambda^2}{c_s^2}z^2, \tag{2.25}$$

where $C = \sqrt{2}D(\sqrt{\eta_*})$. To this accuracy, we may choose λ such that the ions reach the ion sound velocity at the boundary of the plasma. Therefore, the rate of ion generation λ becomes

$$\lambda = \frac{2\sqrt{2}c_s D(\sqrt{\eta_*})}{\pi L}. \tag{2.26}$$

Then, the electric potential reduces to a simple expression,

$$-e\phi(z)/T_e = z^2/2L^2, \tag{2.27}$$

and the ion drift velocity in the z-direction within the quasi-neutral plasma is

$$\frac{v_i(z)}{c_s} = \frac{z}{L}, \tag{2.28}$$

such that Eq. 2.23 is satisfied when $z = L$. It should be noted, unlike the exact solution derived above (Eq. 2.23), the velocity of the ions entering the sheath region is exactly Bohm's velocity when the approximate electric potential (Eq. 2.27) is used; this is to simplify further calculations. Since, given this approximation, the electric field is nowhere infinite, we are free to choose the sheath edge to be the location where Bohm's condition is first satisfied.

The exact solution given as well as the approximation made are for the case of a quasi-neutral plasma. If one were to include the space-charge term in Eq. 2.17, then the solution for the electric potential would diverge from the quasi-neutral solution near the sheath region. One major difference is the fact that the electric potential is continuous across the plasma-sheath boundary whereas the exact solution for the quasi-neutral plasma diverges at that boundary. Therefore, it turns out that the approximation made for the electric potential is closer to the solution that includes the space-charge term than the exact solution near the sheath region. In Fig. 2.2, both the exact solution for a quasi-neutral plasma and the approximation made for this project (together with the fluid solution to be given below) are shown; the divergence of the exact solution (which stems from the neglect of the space-charge term) is removed in the approximation.

For the purpose of this thesis, a partially magnetized plasma (magnetized electrons and unmagnetized ions) with $\mathbf{E} \times \mathbf{B}$ field configuration will be assumed with the magnetic field along the z-direction. Then, the ion drift velocity along the magnetic field lines will be assumed to satisfy Eq. 2.28 as it represents the simplest form of the ion drift in the presence of a sheath which simultaneously satisfies quasi-neutrality in the bulk plasma as well as Bohm's condition for a steady sheath.

This theoretical derivation of the steady-state sheath solution, and corresponding electric potential distribution in the plasma, was the standard for several decades until, in the 1960s, several fluid descriptions and numerical integration methods were introduced to attempt to solve the sheath problem with the space-charge term included.

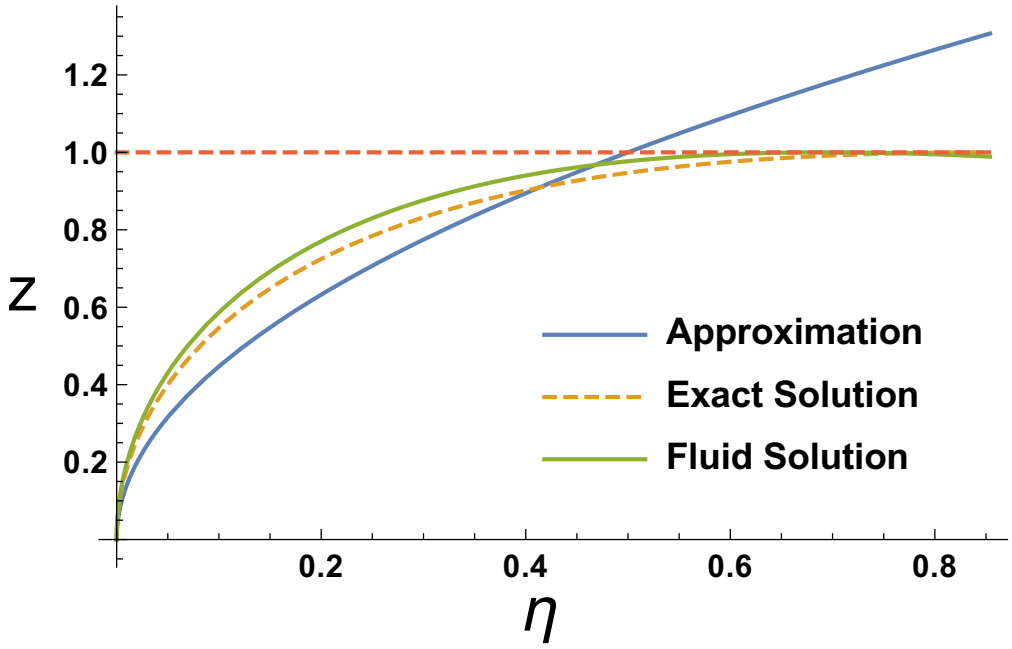

Figure 2.2: Approximate form of the electric potential $-e\phi/T_e = z^2/2L^2$ that satisfies Eq. 2.18 assumed in this project versus the exact solution as well as the fluid solution given in the next section (see Eq. 2.32).

2.3 Numerical & Fluid Solutions

Important contributions to the theory of plasma sheaths were published from 1962 to 1966. The first paper by A. Caruso and A. Cavaliere [18] was pivotal as it lay down the foundations for a full description of the two regions of interest, the quasi-neutral plasma and the space-charge dominated sheath, as well as the transition region. It is the first attempt to provide a full picture of the plasma from the quasi-neutral bulk to the sheath. The general equation to solve is,

$$\lambda_D^2 \frac{d^2}{dz^2}\frac{e\phi(z)}{T_e} = e^{e\phi(z)/T_e} - \frac{1}{\sqrt{2}n_0 c_s}\int_z^L \frac{g(\epsilon)}{\sqrt{e\phi(\epsilon)/T_e - e\phi(z)/T_e}}d\epsilon, \tag{2.29}$$

where $\lambda_D = \sqrt{T_e/4\pi n_0 e^2}$ is the Debye length, L is the length scale of the system and z is measured, here, from the wall (or the electrode) into the plasma. The main idea is to solve the problem in the respective limits by introducing variables for the two different length scales (i.e. $\xi = z/L$ and $\chi = z/\lambda_D$) and then matching the solutions in the transition region which is, by itself, not a trivial task. In the plasma limit, the sheath thickness is negligible

and the Poisson term drops leaving the quasi-neutral integral equation already visited,

$$0 = e^{e\phi(\xi)/T_e} - \frac{1}{\sqrt{2}} \int_{\xi L}^{L} \frac{g(\epsilon)/n_0 c_s}{\sqrt{e\phi(\epsilon)/T_e - e\phi(\xi)/T_e}} d\epsilon. \tag{2.30}$$

In the opposing limit, $\chi = z/\lambda_D$, the Poisson term becomes important and the plasma quasi-neutral bulk region is far removed. Then, in the limit of $\lambda_D \to 0$, one finds,

$$\frac{d^2}{d\chi^2} \frac{e\phi(\chi)}{T_e} = e^{e\phi(\chi)/T_e} - \frac{1}{\sqrt{2}} \int_{0}^{L} \frac{g(\epsilon)/n_0 c_s}{\sqrt{e\phi(0)/T_e - e\phi(\chi)/T_e}} d\epsilon, \tag{2.31}$$

which is a differential equation for $\phi(\chi)$ with boundary condition $\phi(0) = \phi_w$ and $\phi \to \phi(\xi)$ when $\chi \to \infty$; this is the matching condition discussed above. The matching problem is very involved; it was expanded upon by K.-U. Riemann [19] but the problem is yet to be solved. Since the approach in this research project is analytic, an approximate solution will be used based on the assumption that quasi-neutrality applies in the plasma bulk and that the sheath thickness is small. Therefore, as was done in the previous sections, the electric potential in the plasma will be assumed to be parabolic while, in the sheath region, it will satisfy Child-Langmuir's law.

The second paper by S.A. Self [7] considers the exact numerical solution to the integro-differential equation for the electric potential in the plasma (Eq. 2.29). It essentially expands on the theoretical works from his predecessors such as Thompson and Harisson by providing exact numerical values and comparing with the analytical solutions within the plasma bulk (where quasi-neutrality applies) and in the sheath region where ion generation and electron density are neglected. Other than providing an exact numerical solution everywhere for the electric potential, the paper provides insight into the shape of the potential and electric field when the plasma is at steady-state for different ion generation mechanisms.

It should be noted from Fig. 2.3 that the electric potential at the sheath position is slightly less than that predicted from a quasi-neutral plasma and the electric field there is finite. In the case of uniform ion generation rate, Self found that, for $\lambda_D/L \approx 3\%$, the electric potential, normalized by the electron temperature, reduces to about 0.55 whereas our approximate solution gives $-e\phi(L)/T_e = 0.5$. Therefore, our approximate solution for the electric potential is closer to the exact numerical solution including the Poisson term. It

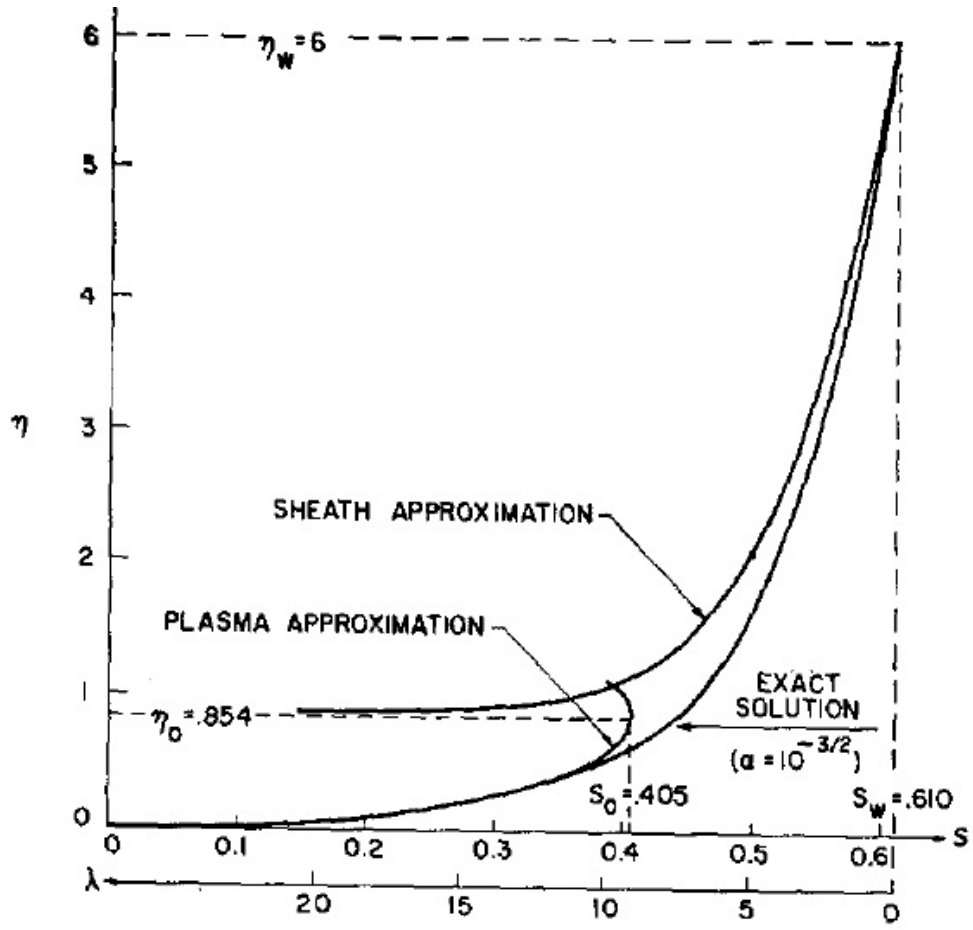

Figure 2.3: Normalized electric potential versus normalized position [7]. Here, the ionization is proportional to the electron density, so that the sheath position $s_0 = 0.405$ instead of $s_0 = 0.344$.

should be noted that ions may be generated through ion-neutral or electron neutral ionization collisions; in this thesis, it will be assumed that electrons are collisionless and that ions are generated at a uniform rate through ion-neutral collisions within the plasma.

Finally, the paper by G.S. Kino and E.K. Shaw [20] provide a different approach to the sheath problem by transforming the kinetic equations into the different moment equations yielding a fully fluid description of the problem. The problem still solves for the electric potential in a quasi-neutral plasma with ion generation, but the solution is found more easily by selecting a small number of moment equations (e.g. neglecting or including pressure terms). For the planar case, uniform ion generation and neglecting the ion pressure (as assumed in this project) one finds readily,

$$\frac{\lambda z}{\sqrt{2}c_s} \approx e^{-\eta}\sqrt{\frac{1}{2}(e^{\eta}-1)}, \tag{2.32}$$

which is much more simple to work with then the exact solution (equation 2.7) and it is readily invertible to find $\eta(z)$. This solution, however, cannot be used in this project as the steady-state for the plasma bulk since it includes the electric field singularity at the sheath boundary (due to the neglect of the space-charge term) which is non-physical. To arrive at a meaningful, albeit approximate, boundary condition to a confined plasma, it is necessary to include only an approximate solution to the zeroth-order fields which does not have any singularity. Expanding Eq. 2.32, one finds the same approximate solution given by Eq. 2.25.

2.4 The State of Plasma Sheath Theory Today

The reference for plasma sheath theory in recent decades as been the review article by K.-U. Riemann [19]. It represents a thorough review of major works on the subject as well as the personal contributions of Riemann which provide insight into Bohm's condition and its generalization when space-charge is included. Further, the author includes source terms for the electrons and ions within the sheath region not included by his predecessors. Finally, the paper provides a thorough analysis of the transition layer and a review of the matching parameters between the sheath and plasma bulk.

Ignoring any ion generation within the plasma, it is possible to derive a differential equation for the electric potential which includes space-charge formation, the result being

$$\left(\frac{e\phi(z)'}{T_e}\right)^2 = 2\frac{m_i v_0^2}{T_e}\left(\sqrt{1-\frac{2e\phi(z)}{m_i v_0^2}}-1\right) + 2\left(e^{e\phi(z)/T_e}-1\right), \tag{2.33}$$

where the subscript 0 refers to the sheath boundary. Unfortunately, this cannot be solved analytically using conventional techniques. However, qualitative results may be seen from Eq. 2.33. Since the left-hand side is strictly positive, the right-hand side must satisfy the condition, to second-order in $e\phi/T_e$,

$$v_0^2 > T_e/m_i = c_s^2, \tag{2.34}$$

which is Bohm's condition. The origin of this condition lies in the ion and electron densities. Since the sheath region is essentially positive, the ion density must be larger than the electron density in this region. Then, because the electron density decreases exponentially with the electric potential and the ion density decreases due to acceleration of the ions into the sheath, the ion flow velocity must be such that the ion density decreases more slowly than the electron density in the sheath region; thus, one finds Bohm's condition. For a plasma at rest far from the sheath regions, a non-zero electric field must, as explained earlier, extend into the plasma from the sheath boundary; this region is referred to as the presheath.

The presheath as been the subject of much debate since it depends on the physical situation. From the ion continuity equation, the assumption of isothermal electrons and quasi-neutrality, one has,

$$\frac{n_i}{n_0} = \sqrt{\frac{m_i}{2T_e}}\frac{n_i v_i}{n_0}\sqrt{\frac{2T_e}{m_i v_i^2}} \equiv j_i\sqrt{\frac{2T_e}{m_i v_i^2}} = n_0 e^{-e\phi/T_e}, \tag{2.35}$$

$$\frac{1}{j_i}\frac{dj_i}{dz} = \frac{c_s}{v_i}\frac{d}{dz}\frac{v_i}{2c_s} - \frac{d}{dz}\frac{e\phi}{T_e}. \tag{2.36}$$

Since, in the presheath, Bohm's condition ($v_i = c_s$) is not satisfied yet, the following inequality must hold,

$$\frac{1}{j_i}\frac{dj_i}{dz} > \frac{d}{dz}\left(\frac{v_i}{2c_s} - \frac{e\phi}{T_e}\right). \tag{2.37}$$

Comparing with the ion equation of motion, the right-hand side must vanish identically; the ion flux density must then increase with z. Now, depending on the assumptions taken in the plasma, several different relationships between the ion flow and the electric potential are possible which satisfy this inequality; several examples are given in Ref. [19]. A geometrical presheath, for example, would have an increasing ion current density due to the curvature of the bounding wall [19]; then, the right-hand side of inequality 2.37 is strictly positive. In a collisional presheath, ions are retarded by a frictional force due to ion-neutral and/or ion-electron collisions; the left-hand side of the inequality is then negative since the electric force must, necessarily, be bigger than the change in momentum of the ions. For the an ionizing presheath, there is a combination of ion friction as well as increasing ion current density; the inequality 2.37 is then satisfied due to the same reasons as the previous two examples.

In this thesis, the presheath will be assumed to be of the ionization type, the ionization rate being uniform within the plasma. However, the ion-neutral collisions assumed to be at the origin of the ion generation will be neglected in the perturbed equations for the ions, assumed to be of much smaller magnitude than the electric force and ion inertia.

Chapter 3

Classical Instabilities in Cold Plasmas

Plasmas are complex structures exhibiting an extremely diverse set of behaviours at varying scales, from the very small (micro-instabilities in inertial fusion devices) to the very large (space plasmas including solar winds and the Earth's magnetosphere). Because plasmas are made of an ensemble of positive and negative elements (such as ions and electrons) and these interact over macroscopic distances, any given particle will interact with all other particles in the plasma. Therefore, plasmas will exhibit large-scale, collective behaviours not seen in neutral fluids. This makes the dynamics of plasmas much more intricate and rich leading to energy exchange over scales spanning several orders of magnitude. Then, whenever a source of energy is present in a plasma (such as an electron beam injected into a steady plasma or field gradients) unstable oscillations may be excited in the plasma called instabilities that may feed on the energy source and increase in magnitude. Depending on the specific electric and magnetic field configuration in a plasma as well as the parameters of the plasma (temperature, number density, etc.), several assumptions need to be made leading to a set of fluid equations that describe different types of linear instabilities over varying time and length scales.

In the following chapter, we will first look into the main assumptions for this research project, starting from the general kinetic description of a plasma and reducing it to a set of fluid equations suitable for a partially magnetized $\mathbf{E} \times \mathbf{B}$ plasma. Assuming that the quantities described by the fluid equations (velocity, electric potential, density, etc.) are slightly perturbed from their equilibrium values, then one assumes the perturbed quantities are small and that $\tilde{\Phi} \sim \tilde{v} \sim \tilde{n} \sim e^{i\mathbf{k}\cdot\mathbf{r}-i\omega t}$. Then, two important instabilities that may exist (under certain conditions) in this plasma configuration, the Simon-Hoh instability and the resistive instability, will be derived from the first-order equations in the small perturbations.

These will be important later in the description of the stability of bounded Hall plasmas.

3.1 Fluid Equations

The most general description of a plasma must necessarily involve every single constituent particles (e.g. electrons, ions and neutrals). Ideally, one would follow every single particle from its initial position and velocity and, through summing up its interaction with every other particle as well as with any externally applied electric and magnetic fields, trace out its path through phase space. This approach, however, is very time consuming and requires a lot of computing resources. The dynamics of a plasma may be made more tractable by taking an average over the specific ensembles; for example, averaging of the ion species, the electron species and the neutral species. In doing so, however, one introduces a collisional term which takes into account the change in the distribution function that may arise from collisions between particles (both within a species or between species). Then, the distribution function for a given species σ is $f_\sigma(\mathbf{x}, \mathbf{v}, t)$ and must satisfy the equation,

$$\frac{\partial f_\sigma}{\partial t} + \mathbf{v} \cdot \nabla f_\sigma + \mathbf{a} \cdot \nabla_v f_\sigma = C_\sigma, \tag{3.1}$$

where $\mathbf{a} = q(\mathbf{E} + \mathbf{v} \times \mathbf{B}/c)/m$, q is the particle charge, m its mass and the collisional term C_σ is given by,

$$C_\sigma = \sum_{\sigma'} \int v_{rel}(f'_\sigma f'_{\sigma'} - f_\sigma f_{\sigma'}) d\Omega d^3\mathbf{v}, \tag{3.2}$$

where $d\Omega$ refers to the differential solid angle into which a particle is scattered from a collision with another particle. Eq. 3.1 is referred to as Boltzmann's equation. Here, f_σ is the average distribution function over species σ (i.e. electrons, ion or neutrals). This equation is, however, still too complex as it involves six variables (for position and velocity) and include phenomena on all scales of length and time. In order to start to simplify the analysis, one may take moments in the velocity variable to effectively reduce the equation to a set of equations in three variables. Integrating, in the velocity variables after multiplying, respectively, by m_σ, $m_\sigma \mathbf{v}_\sigma$ and $m_\sigma v_\sigma^2/2$ (mass, momentum and energy), one finds,

$$\frac{\partial n_\sigma}{\partial t} + \nabla \cdot (n_\sigma \mathbf{V}_\sigma) = 0, \tag{3.3}$$

$$m_\sigma n_\sigma \frac{\partial \mathbf{V}_\sigma}{\partial t} + m_\sigma n_\sigma (\mathbf{V}_\sigma \cdot \nabla)\mathbf{V}_\sigma + \nabla \cdot \bar{\bar{\mathbf{\Pi}}}_\sigma - n_\sigma e_\sigma (\mathbf{E} + \mathbf{V}_\sigma \times \mathbf{B}/c) = \mathbf{F}_\sigma, \tag{3.4}$$

$$\frac{\partial}{\partial t}\left(\frac{3}{2}P_\sigma + \frac{1}{2}m_\sigma n_\sigma V_\sigma^2\right) + \nabla \cdot \mathbf{q}_\sigma - e_\sigma n_\sigma \mathbf{E} \cdot \mathbf{V}_\sigma = W_\sigma + \mathbf{V}_\sigma \cdot \mathbf{F}_\sigma, \tag{3.5}$$

$$\sum_{\sigma'} \int m_\sigma \mathbf{v}_\sigma C_{\sigma\sigma'} d^3\mathbf{v} = \mathbf{F}_\sigma, \tag{3.6}$$

$$\sum_{\sigma'} \int \frac{1}{2} m_\sigma \mathbf{v'}_\sigma^2 C_{\sigma\sigma'} d^3\mathbf{v} = W_\sigma, \tag{3.7}$$

where e_σ is the charge of the particle, $n_\sigma = \int f_\sigma d^3\mathbf{v}_\sigma$ is the number density, $n_\sigma \mathbf{V}_\sigma = \int \mathbf{v}_\sigma f_\sigma d^3\mathbf{v}_\sigma$ is the average flux (i.e. $\mathbf{v}_\sigma$ is velocity of species σ), $\bar{\bar{\mathbf{\Pi}}}_\sigma = \int \mathbf{v}_\sigma \mathbf{v}_\sigma f_\sigma d^3\mathbf{v}_\sigma$ is the momentum flux tensor and $\mathbf{q}_\sigma = \frac{1}{2}\int m_\sigma v_\sigma^2 \mathbf{v}_\sigma f_\sigma d^3\mathbf{v}_\sigma$ is the average heat flux. Further, we assumed that $\mathbf{v}_\sigma = \mathbf{V}_\sigma + \mathbf{v}'_\sigma$ (i.e. the velocity of any given particle of species σ is the sum of its flow velocity and random (thermal) velocity); then, because $\overline{\mathbf{v}'_\sigma \mathbf{v}'_\sigma}$ is a symmetric tensor of rank 2, it is equivalent to $\mathbf{I}\overline{v'^{\,2}_\sigma}/3$, $\overline{v'^{\,2}_\sigma} \equiv 3T_\sigma/m_\sigma = 3P_\sigma$. The energy equation may then be simplified further by re-writting $\bar{\bar{\mathbf{\Pi}}}_\sigma = \bar{\bar{\boldsymbol{\pi}}}_\sigma + P_\sigma \bar{\bar{\mathbf{I}}}$ where $\bar{\bar{\boldsymbol{\pi}}}_\sigma$ is the advection tensor related to the average flow (i.e. $\bar{\bar{\boldsymbol{\pi}}}_\sigma \equiv \pi_\sigma^{ij} = n_\sigma V_\sigma^i V_\sigma^j$) and P_σ is the fluid isotropic pressure whilst using the equation of motion and continuity to yield,

$$\frac{3}{2}\frac{dP_\sigma}{dt} + \frac{5}{2}P_\sigma \nabla \cdot \mathbf{V}_\sigma + \bar{\bar{\boldsymbol{\pi}}}_\sigma : \nabla \mathbf{V}_\sigma + \nabla \cdot \mathbf{q}_\sigma = W_\sigma, \tag{3.8}$$

where, in component form, $\bar{\bar{\boldsymbol{\pi}}}_\sigma : \nabla \mathbf{V}_\sigma \equiv \pi_\sigma^{ji} \nabla_i V_j$. It should be mentioned that the viscosity tensor which is proportional to $\nabla \mathbf{V}_\sigma$ was dropped in the momentum flux tensor $\bar{\bar{\mathbf{\Pi}}}_\sigma$ since, as mention in Ref. [21], this term would provide a force which is of the same order as the inertia term which was already neglected. These equations are incomplete because we have yet to determine the form of the collisional terms $C_{\sigma\sigma'}$ which depend on the type of collisions between the electrons, ions and neutrals. In Hall thrusters, the ions are cold and unmagnetized while the electrons are hot and magnetized; therefore, the energy equation for the ions can be drop entirely and the pressure gradient term in the equation of motion is neglected. The electron-ion collisions are also neglected since the collision frequency is inversely proportional to $T_e^{3/2}$ and it is already assumed to be significant.

The friction term between the ions and neutrals F_i will be neglected in thesis; this may be motivated by the fact that the ions are cold and have non-zero velocity only near the sheath region. Further, electron-neutral collisions will be neglected; this is because we will assume that the electrons are free to move to maintain, at steady-state, a Boltzmann distribution along the magnetic field lines. Finally, because of the smallness of the ratio $m_e/m_{i,n}$, the energy lost in any given collision is negligible; then, we may neglect the terms W_e and $\mathbf{V}_e \cdot \mathbf{F}_e$. The equations for the ions then simplify to,

$$\frac{\partial n_i}{\partial t} + \nabla \cdot (n_i \mathbf{V}_i) = 0, \tag{3.9}$$

$$m_i \frac{d\mathbf{V}_i}{dt} - e\mathbf{E} = 0, \tag{3.10}$$

and the electrons to,

$$\frac{\partial n_e}{\partial t} + \nabla \cdot (n_e \mathbf{V}_e) = 0, \tag{3.11}$$

$$m_e n_e \frac{d\mathbf{V}_e}{dt} + \nabla \cdot \bar{\bar{\mathbf{\Pi}}}_e + n_e e(\mathbf{E} + \mathbf{v}_e \times \mathbf{B}/c) = 0, \tag{3.12}$$

$$\frac{3}{2}\frac{dP_e}{dt} + \frac{5}{2}P_e \nabla \cdot \mathbf{V}_e + \bar{\bar{\boldsymbol{\pi}}}_e : \nabla \mathbf{V}_e + \nabla \cdot \mathbf{q}_e = 0. \tag{3.13}$$

The next important assumption is now made. Since we are interested in phenomena much slower than the electron transit time along the magnetic field lines, we may assume that electrons are distributed isothermally at any given point in time. Then, the energy equation for the electrons reduces to $P_e/n_e = Const$ (i.e. isothermal gas condition). Further, we will neglect the electron inertia term. The final set of equations that will be considered in this project is thus,

$$\frac{\partial n_i}{\partial t} + \nabla \cdot (n_i \mathbf{V}_i) = 0, \tag{3.14}$$

$$m_i \frac{d\mathbf{V}_i}{dt} - e\mathbf{E} = 0, \tag{3.15}$$

$$\frac{\partial n_e}{\partial t} + \nabla \cdot (n_e \mathbf{V}_e) = 0, \tag{3.16}$$

$$\nabla P_e + n_e e(\mathbf{E} + \mathbf{v}_e \times \mathbf{B}/c) = 0, \tag{3.17}$$

where the term in $\bar{\bar{\boldsymbol{\pi}}}$ was dropped since we assume the electron have uniform $\mathbf{E} \times \mathbf{B}$ drift.

In this thesis, we will investigate the dynamics of a Hall plasma (a plasma made of cold, unmagnetized ions and warm, magnetized electrons with a $\mathbf{E} \times \mathbf{B}$ field configuration). It is well known that, in the presence of an externally applied electric field perpendicular to a magnetic field, a density gradient will form leading to the Simon-Hoh instability. Therefore, before investigating how sheaths affect this plasma instability, it is worth reviewing it.

3.2 Simon-Hoh Instability

In 1963, Albert Simon published the paper that first introduced the field to what would henceforth be referred to as the Simon-Hoh instability [22]. The author used a slab plasma geometry with an $\mathbf{E} \times \mathbf{B}$ field configuration. At steady-state (i.e. when the system relaxes to a state independent of time) with $\mathbf{E}_0 = E_0 \mathbf{x}$, the ion and electric currents perpendicular to the magnetic field are given by

$$\mathbf{j}_{\perp,i/e} = -D_{\perp,i/e} \frac{dn_0}{dx} \pm n_0 \mu_{\perp,i/e} E_0 \tag{3.18}$$

where $\mu^{\pm}$ and $D_{\pm}$ are, respectively, the mobility and diffusion coefficients of the ions and electrons across the magnetic field lines. At steady-state, the continuity equations for the ions and electrons,

$$\nabla \cdot \mathbf{j}_{\perp,i/e} = 0, \tag{3.19}$$

yield,

$$\nabla \cdot \mathbf{j}_{\perp,i} = -\frac{D_{\perp,i}}{\mu_{\perp,i}} \frac{d^2 n_0}{dx^2} + \frac{d}{dx}\left(n_0 E_0\right) = 0, \tag{3.20}$$

$$\nabla \cdot \mathbf{j}_{\perp,e} = -\frac{D_{\perp,e}}{\mu_{\perp,e}} \frac{d^2 n_0}{dx^2} - \frac{d}{dx}\left(n_0 E_0\right) = 0. \tag{3.21}$$

Adding the two equations, one finds,

$$\left(\frac{D_{\perp,i}}{\mu_{\perp,i}} + \frac{D_{\perp,e}}{\mu_{\perp,e}}\right) \frac{d^2 n_0}{dx^2} = 0. \tag{3.22}$$

Therefore, the number density $n_0 = \frac{A(L-x)}{L} + C$ is a linear function of x (the form chosen here is for convenience) where A and C are constants of integration and L is the length scale of the system along the perpendicular direction to the magnetic field. From either continuity equation, it is not clear that $n_0 E_0 = \text{const}$ (assuming the mobility of the ions or electrons is uniform). Then, we get the steady-state solutions for the number density and electric field,

$$n_0(x) = \frac{A(L-x)}{L} + C, \tag{3.23}$$

$$E_0(x) = -\frac{A}{L}\frac{\phi}{ln\left(\frac{A+C}{C}\right)(A(L-x)/L + C)}, \tag{3.24}$$

where ϕ is the electric potential difference applied externally; note that we are free to set the potential drop to be positive or negative. Therefore, given an externally applied electric field, there will be a gradient in density induced in the plasma in the direction of the applied field.

Neglecting the electron inertia, we have, from the equations of motion of the ions and electrons,

$$0 = \frac{\partial}{\partial z}\left(\frac{e\phi}{T_e} - \ln\left(\frac{n_e}{n_0}\right)\right), \tag{3.25}$$

$$\mathbf{j}_{e,\perp} = \frac{en_e v_{Te}^2}{\omega_{ce}}(\mathbf{b}\times\nabla_\perp)\left(\frac{e\phi}{T_e} - \ln\left(\frac{n_e}{n_0}\right)\right) \tag{3.26}$$

$$\mathbf{v}_i = \frac{iec_s^2}{\omega}\nabla\frac{e\phi}{T_e}. \tag{3.27}$$

In order to derive the dispersion equation for waves in this plasma configuration, one needs to expand the quantities up to first-order. To derive the Simon-Hoh instability, the finite extent of the plasma in the z-direction is neglected. Then, one may Fourier transform the z-direction similarly to the perpendicular directions. One thus finds, from the ion and electron continuity equations,

$$(\omega - \omega_0)\frac{\tilde{n}_e}{n_0} + \omega_*\frac{e\tilde{\Phi}}{T_e} = 0, \tag{3.28}$$

where $\omega_0 = -k_y v_{Te}^2 E_0/\omega_{ce}$ is the electron drift frequency and $\omega_* = -k_y v_{Te}^2/\omega_{ce}L_n$ and $L_n^{-1} = (1/n_0)d(n_0)/dz$. The ions, on the other hand, must satisfy the following equation,

$$\frac{\tilde{n}_i}{n_0} + \frac{c_s^2 k^2}{\omega^2}\frac{e\tilde{\Phi}}{T_e} - \frac{ic_s^2 k_x}{\omega^2 L_n}\frac{e\tilde{\Phi}}{T_e} = 0. \tag{3.29}$$

Using quasi-neutrality, we finally arrive at the dispersion equation,

$$(\omega - \omega_0)\,\frac{c_s^2(k^2 - ik_x L_n^{-1})}{\omega^2} - \omega_* = 0, \tag{3.30}$$

where a complex-valued solution to ω exists with a positive imaginary part (growth rate) when $\nabla n_0 \cdot \mathbf{E}_0 > 0$; then, an instability exists. The main result may be summarized as follows. Given a static electric field and a density gradient parallel to it, the build up of charge induced by the imbalance in cross-magnetic field drifts for the unmagnetized ions and magnetized electrons creates an instability that grows with time, proportional to the electric field and density gradient.

The Simon-Hoh instability is very important in this project since it is present in plasma devices of the type considered here. Therefore, it will be referred to often. Further, it will be shown that this instability is modified by the presence of sheaths in the next chapter.

3.3 Resistive Instability

The resistive instability exists when electrons undergo collisions (with ions are neutrals). In such a case, an added term related to the change in momentum of an electron in any given collision is introduced in the equation of motion of the electrons. Assuming, for simplicity, that there are only electron-neutral collisions along the magnetic field (i.e. in the z-direction) and that the electron cyclotron frequency ω_{ce} is much larger than the oscillation frequency, we have the set of equations for the perturbed quantities,

$$\begin{aligned} m_e(\omega + i\nu)v_{ez} &= -ek_z\phi + T_e k_z \frac{n_e}{n_0}, & (3.31)\\ \mathbf{v}_{e\perp} &= \frac{v_{Te}^2}{\omega_{ce}}\left(\frac{n_e}{n_0} i\mathbf{k}_\perp \times \mathbf{z} - \frac{e\phi}{T_e} i\mathbf{k}_\perp \times \mathbf{z}\right), & (3.32)\\ (\omega - \omega_0)n_e - n_0\mathbf{k}\cdot\mathbf{v}_e &= 0, & (3.33) \end{aligned}$$

where, as before, the ω_0 is the drift frequency of the electrons in the $\mathbf{E}\times\mathbf{B}$ field configuration. The ions equation of motion and continuity are simply,

$$m_i \omega \mathbf{v}_i = e\mathbf{k}\phi, \tag{3.34}$$

$$\omega n_i - n_0 \mathbf{k} \cdot \mathbf{v}_i = 0. \tag{3.35}$$

Assuming quasi-neutrality, one may combine Eqs. 3.31 through 3.35 and the dispersion equation becomes, after some simplification,

$$\omega^2 + \frac{k^2}{k_z^2}\frac{m_e}{m_i}\left[(\omega - \omega_0)(\omega + i\nu) - k_z^2 v_{Te}^2\right] = 0. \tag{3.36}$$

The collisional term then adds an imaginary term to the dispersion equation. Therefore, under the right conditions, the imaginary part of the angular frequency ω is positive and an instability exists.

This type of instability will be compared to the instability that exists when we include sheaths since, in the next chapter, it will be shown that the two instabilities are similar in form.

Chapter 4

Modification of the Simon-Hoh Instability by Sheath Effects in Partially Magnetized Hall Plasmas

The main goal of this chapter is to demonstrate how the presence of sheaths affect significantly the stability of bounded Hall plasmas. Even when the Simon-Hoh condition for instability ($4v_0v_*/c_s^2 > 1$) is not yet satisfied, it may still exist under the right conditions when the sheath boundary condition is included. It will be shown that the sheath restricts the ion current, and therefore the electron current through conservation of charge at the boundaries, and behaves like a resistive term in the dispersion equation. This chapter provides an approximate solution to the problem of a bounded Hall plasma under the assumption that $k_z^2 \ll k_y^2$. This chapter is based on a paper published in the peer-reviewed journal Physics of Plasmas [2].

4.1 Introduction

Plasma discharges based on $\mathbf{E} \times \mathbf{B}$ fields are used in a variety of applications for electric propulsion and plasma processing. In applications as Hall thruster, Penning traps and magnetron devices, the plasmas are only partially magnetized; the electrons being magnetized while the ions are not. In such such plasmas the electric field perpendicular to the external magnetic field is often used to confine electrons and support the discharge. When the plasma density is inhomogeneous across the magnetic field, as is expected for magnetically confined electrons, the electron drift together with the inertial response of unmagnetized ions result in

an peculiar eigen-mode of partially magnetized plasmas: the so-called "anti-drift" mode [23]. This mode is a basis for various extensions and instabilities existing in a partially magnetized plasma, which are generically referred here as gradient-drift modes [24, 21, 25]. The simplest expression for the anti-drift mode frequency is given by

$$\omega \equiv \frac{k^2 c_s^2}{\omega_*} = -k_y L_n \omega_{ci}, \tag{4.1}$$

where k_y refers to the perpendicular wave-vector, $c_s = \sqrt{T_e/m_i}$, $\omega_* = -c_s^2 k_y / L_n \omega_{ci}$, $\omega_{ci} = eB_0/m_i c$ is the ion cyclotron frequency (assuming singly-charge ions) and $L_n^{-1} = (dn/dx)/n$ is the inverse density gradient length scale.

For the Hall thruster geometry consider a small region of the plasma which is approximately planar (i.e. we set the radius of curvature characteristic of the system to be very large) and we set the axial direction to be the x-direction, the y-direction to be along the azimutal direction and the z-direction to be in the radial direction. Then, k_y is the component of the wave-vector along the azimuthal direction which is periodic. Similar approximations can be made for the magnetron and Penning discharge geometries, so we assume that the y-direction is always periodic, z-direction is along the magnetic field, and x-direction is the direction of the density gradient and the electric field. It should be noted that this mode occurs for $k_z = 0$. [1]

The $\mathbf{E} \times \mathbf{B}$ plasma discharges are supported by the energy input from the externally imposed electric field $\mathbf{E}_0 = E_0 \mathbf{x}$ which causes the equilibrium electron $\mathbf{E}_0 \times \mathbf{B}_0$-drift where $\mathbf{B}_0 = B_0 \mathbf{z}$. The Doppler shift due to the electron drift, $\mathbf{v}_0 = cE_0/B_0 \mathbf{y}$, results in the modification of the electron response with $\omega \to \omega - k_y v_0 = \omega - \omega_0$ in the electron continuity equation whereas the ion continuity equation retains a term in ω. The dispersion relation becomes,

$$\frac{k^2 c_s^2}{\omega^2} = \frac{\omega_*}{\omega - \omega_0}, \tag{4.2}$$

and, therefore, producing the reactive instability of the anti-drift mode if the condition

[1] The mode was originally called the anti-drift mode [22] because of the inverse dependence on the electron drift frequency. Note, however, that this mode is significantly different from the standard drift waves of fully magnetized plasmas and in fact does not depend on the electron temperature.

$4v_0v_* > c_s^2$ is met. This implies a condition on the density gradient and externally applied electric field, $E_0(dn/dx) > 0$. This instability, referred to as the collisionless Simon-Hoh instability, is one of several instabilities existing in Hall plasmas [26, 21]. In the simplest case, this instability and resulting plasma dynamics are often considered in neglect of the electron motion along the magnetic field or assuming periodicity in this direction. It is our goal to consider finite and bounded plasmas where the magnetic field lines are intercepted by material walls. In this case, the sheaths formed at the boundaries become important and constrain the parallel plasma motion. It will be seen that this induces a dissipative-type instability.

That there exist instabilities enabled by the sheath with wavelengths of the order of the system length was first shown in Refs. [27, 28]. Shear flow and temperature-gradient instability driven by the sheath were studied in application to the divertor and scrape-off layer in tokamaks. The sheath driven instability due to the electron secondary emission was shown in Ref. [29]. All of these works were performed under the assumption of fully magnetized plasmas. Sheath effects on the modes in partially magnetized plasma were investigated in Ref. [25], but in neglect of the plasma density gradient.

It turns out that the effect of the sheath is similar in structure to the effect of electron motion along the magnetic field in the presence of the electron-neutral collisions. Thus, we will review this case first. Then, the appropriate boundary conditions for our problem will be presented and used to derive the dispersion equation for the case of the collisionless, bounded plasma. The following section will demonstrate the modification of the condition for the classical Simon-Hoh instability due to the presence of finite resistivity and then expose the two main limiting cases (e.g. $v_0 = 0$ and $v_* = 0$). Finally, the system with both electron drift and ion density gradient will be analyzed and it will be shown that the growth rate (as well as the angular frequency of the plasma oscillation modes) are significantly modified by the presence of finite resistivity, would it be due to neutral-electron collisions or due to the conservation of current at the bounding walls.

4.2 Governing Equations

The equation of motion for the electrons, neglecting electron inertia, is given by

$$0 = -e\left(-\nabla\Phi + \frac{\mathbf{v}_e}{c}\times\mathbf{B}\right) - \frac{\nabla(n_e T_e)}{n_e} - \nu m_e v_{ez}\mathbf{z}. \tag{4.3}$$

Linearizing equation 4.3 for small perturbations in the electric potential, number density and velocity yields the set of equations,

$$\frac{\nu}{v_{Te}^2}\tilde{v}_{ez} = \frac{\partial}{\partial z}\left(\frac{e\tilde{\Phi}}{T_e} - \frac{\tilde{n}_e}{n_0}\right), \tag{4.4}$$

$$\tilde{\mathbf{v}}_{e\perp} = \frac{c\mathbf{b}\times\nabla_\perp\tilde{\Phi}}{B_0} - \frac{cT_e\mathbf{b}\times\nabla_\perp\tilde{n}_e}{n_0 eB_0}. \tag{4.5}$$

Assuming, because of the periodicity in $\mathbf{y}$ and the infinite extend in $\mathbf{x}$, the form $(\tilde{\Phi},\tilde{n}) \sim e^{-i\omega t + i\mathbf{k}_\perp\cdot\mathbf{r}_\perp}$, it is easy to show that,

$$(\omega-\omega_0)\frac{\tilde{n}_e}{n_0} - \omega_*\frac{e\tilde{\Phi}}{T_e} + i\frac{\partial\tilde{v}_{ez}}{\partial z} = 0. \tag{4.6}$$

The equation of motion for the unmagnetized ions is given by,

$$\frac{\partial\mathbf{v_i}}{\partial t} + (\vec{v}_i\cdot\nabla)\mathbf{v}_i = -\frac{e}{m_i}\nabla\Phi. \tag{4.7}$$

Then, to first-order in the perturbation $\tilde{\Phi} = \tilde{\Phi}(z)e^{-i\omega t + i\mathbf{k}_\perp\cdot\mathbf{r}_\perp}$ we have,

$$\tilde{v}_{iz} = \frac{e}{i\omega m_i}\frac{\partial\tilde{\Phi}}{\partial z}, \tag{4.8}$$

$$\tilde{\mathbf{v}}_{i\perp} = \frac{e}{m_i\omega}\mathbf{k}_\perp\tilde{\Phi}. \tag{4.9}$$

The continuity equation for the ions then yields,

$$-i\omega\frac{\tilde{n}_i}{n_0} + i\mathbf{k}_\perp\cdot\tilde{\mathbf{v}}_{i\perp} + \frac{\partial\tilde{v}_{iz}}{\partial z} = 0. \tag{4.10}$$

Assuming quasi-neutrality as well as taking $\partial/\partial z \to ik_z$, one finds the dispersion equation,

$$\frac{\omega_* + ik_z^2 v_{Te}^2/\nu}{\omega-\omega_0+ik_z^2v_{Te}^2/\nu} = \frac{k^2c_s^2}{\omega^2}, \tag{4.11}$$

which was shown for a plasma of unmagnetized ions and non-vanishing k_z [26, 23]. It should be noted that a similar problem was considered in Refs [30, 31], but the parallel electron velocity was taken in the form of an ambipolar diffusion flux rather than in the form of equations 4.4 and 4.5. In fact, the self-consistent density response is constrained by the quasi-neutrality condition where both parallel and perpendicular electron velocities are responsible for maintaining quasi-neutrality.

4.3 Results & Analysis

In many physical situations, it is interesting to look at large scale perturbations along the magnetic field lines since these modes are constrained by the boundary conditions at the bounding walls. Then, k_z is much smaller than k_y (it is implicitly assumed that perturbations in the x-direction are similar to the length scale of the system (i.e. $k_x^2 \sim k_z^2 \ll k_y^2$)). Since the **z**-direction is finite, the eigen-functions of the system will be the solution of a differential equation in z; it is then necessary to determine the boundary conditions along the magnetic field. These boundary conditions are determined by the dynamics of the electrons and ions in the sheath region. The standard sheath model for a planar, quasi-neutral plasma will be assumed. Therefore, the walls will be fully absorbing, the plasma-sheath boundary will be defined as the location where the ions reach Bohm's velocity c_s and the electron will be distributed isothermally (i.e., Boltzmann distribution) along the magnetic field being mostly reflected by the strong electric field in the sheath region. Since, at steady-state, there is no net current entering the sheath, the net current density vanishes,

$$J_{sh,0} = 0 = J_{0i} + J_{0e} = en_0 c_s - \frac{en_0 v_{Te}}{\sqrt{2\pi}} e^{-e\phi_{sh}/T_e}, \tag{4.12}$$

where $e\phi_{sh}/T_e > 0$ is the equilibrium plasma potential at the sheath entrance (with respect to the wall potential). It is straightforward to solve for the normalized electric potential, the result being, for a singly-charged Xenon plasma, $-e\phi_{sh}/T_e = \ln(2\pi m_e/m_i)/2 \approx 5$. Since the plasma density and electric potential perturbations will perturb the electron current entering the sheath, one finds, for small perturbations,

$$\tilde{J}_{ez}(L) = en_0 c_s \left(\frac{e\tilde{\Phi}(L)}{T_e} - \frac{\tilde{n}_e(L)}{n_0} \right). \tag{4.13}$$

This provides us with a boundary condition on the electron current density at the plasma-sheath interface ($z \approx L$). Using the ion density response and quasi-neutrality in the bulk plasma, one finds the simple form for equation 4.13,

$$\tilde{J}_{ez}(L) = en_0 c_s \frac{e\tilde{\Phi}(L)}{T_e} \left(1 - \frac{k_y^2 c_s^2}{\omega^2} \right). \tag{4.14}$$

This boundary conditions can be implemented into equation 4.6 by averaging over z from $-L$ to L whilst assuming the density perturbation is even in z,

$$(\omega - \omega_0)\frac{\tilde{n}_e}{n_0} - \omega_* \frac{e\tilde{\Phi}(L)}{T_e} = i\frac{1}{en_0 L}\tilde{J}_{ez}(L). \tag{4.15}$$

Again, using quasi-neutrality as well as the ion density we have,

$$\left((\omega - \omega_0)\frac{k_y^2 c_s^2}{\omega^2} - \omega_* \right) \frac{e\tilde{\Phi}(L)}{T_e} = i\frac{c_s}{L}\frac{e\tilde{\Phi}(L)}{T_e} \left(1 - \frac{k_y^2 c_s^2}{\omega^2} \right), \tag{4.16}$$

or, the final dispersion relation,

$$\frac{k_y^2 c_s^2}{\omega^2} = \frac{\omega_* + ic_s/L}{\omega - \omega_0 + ic_s/L}, \tag{4.17}$$

which is similar in structure to the dissipative instability due to electron-neutral collisions seen in equation 4.11. It is worth noting that, in the long wavelength approximation $k_z^2 \ll k_y^2$, the ion current in the **z**-direction can be neglected; thus, there is no contribution to the ion density response from the ion current entering the sheath.

Properties of the dispersion equations 4.11 and 4.17 can be presented in the same form using the notation $\nu_\parallel = c_s/L$ as a characteristic parallel flow frequency in the sheath bound plasma or with $\nu_\parallel = k_z^2 v_{Te}^2/\nu$ as typical parallel diffusion frequency for collisional plasmas. The relative importance of the sheath resistivity over the parallel collisional diffusion for $k_z \simeq 1/L$ is given by the standard condition [32, 33],

$$\lambda/L > \sqrt{m_e/m_i}, \tag{4.18}$$

where $\lambda \equiv v_{Te}/\nu$ is the electron mean free path.

Also, we are interested in low frequency long wavelength instabilities with $\omega < \omega_{LH} = \sqrt{\omega_{ce}\omega_{ci}}$ ($\approx 488\omega_{ci}$ for a Xenon plasma) so that the effects of the lower hybrid mode seen in Ref [21] are neglected. We consider modes with low m (azimuthal mode number), roughly corresponding to the wavelengths of the order of the device radius. For estimates in what follows, we use the $k_y\rho_s \simeq 1$.

Before presenting some results for different limiting cases as well as the modification of the Simon-Hoh instability, it is worth revisiting the physical mechanism behind the resistive instability. In the presence of cross electric and magnetic fields, the electrons will drift along the perpendicular direction to both of these fields. Then, if a small perturbation exists as well as an ion density gradient along this direction, there will be periodic regions of lower and higher density of electrons (relative to the ions) and therefore a fluctuating electric potential will be generated. In a perfectly conducting plasma, the electrons are free to move to lower density regions and thus short-circuit the induced electric field; the drift wave is then purely oscillatory. However, when some agent restricts the free motion of electrons, would it be electron-neutral collisions or the presence of a plasma sheath which restricts the electron current along the magnetic field [27], there will be a phase lag between the electric potential and the density fluctuations. In such a case, the induced $\mathbf{E} \times \mathbf{B}$ drift will actually increase the density fluctuations, exasperating the difference between high and low density regions. The main results which follow provide a quantitative description of the growth rate of this resistive drift instability in different limits.

The collisionless Simon-Hoh instability is recovered in the limit $\nu_\parallel \to 0$. The instability requires the standard condition $4v_0v_* > c_s^2$. However, for a non-zero $\nu_\parallel \neq 0$, the condition is modified, $4(v_0v_* + \nu_\parallel/k_y^2) > c_s^2$, and the dissipation lead to the disappearance of the threshold in v_0 resulting in a weak instability occurring for lower values of v_0 and even in the limit of $v_0 \to 0$ (see Fig. 4.1).

It is of interest to note the instability in absence of the electron drift, $v_0 = 0$, which occurs for finite values of the $\nu_\parallel$ parameter. In this case, the Simon-Hoh instability is not present and the anti-drift mode is destabilized by the dissipation, either from collisions or from the sheath resistivity (see Fig. 4.2). This anti-drift-dissipative mode is the partially magnetized counterpart to the drift-dissipative instabilities existing in fully magnetized plasmas [27, 34].

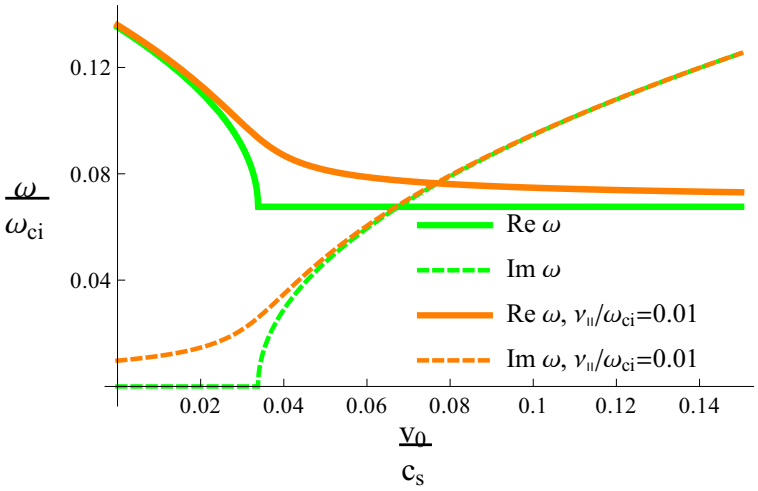

Figure 4.1: The collisionless Simon-Hoh instability and its modification due to the sheath resistivity with $\nu_{\|}/\omega_{ci} = 0.01$ and $k_y\rho_s = 1$ when the threshold for the instability disappears [2]. It should be mentioned that the normalization constant used here, the ion cyclotron frequency ω_{ci}, is used since it is related to the electron cyclotron frequency (an important frequency constant of a Hall plasma) and the proportionality constant $(\sqrt{m_e/m_i})$ is more convenient for the representation of the results.

In the limit of small $\nu_{\|}$, the growth rate vanishes and the real part of the mode frequency converges to $k_\perp c_s/\omega_*$ as expected from the equations 4.11 and 4.17. For larger values of $\nu_{\|} \gg (\omega_*, \omega_0)$ the dispersion equation (4.17) predicts the weakly unstable ion sound mode $\omega^2 \simeq k_y^2 c_s^2$ with the growth rate decaying as $\gamma \sim \nu_{\|}^{-1}$.

$$\omega = \frac{(k_y c_s)^2}{2(\omega_* + i\nu_z)} \left(1 + \sqrt{1 + \frac{i4\nu_z}{(k_y c_s)^2}(\omega_* + i\nu_z)} \right). \tag{4.19}$$

Alternatively, in the case of vanishing $v_* = 0$, one finds the instability which is driven by the electron drift and the finite resistivity. The growth rate decays for large $\nu_{\|}$ and vanishes for $\nu_{\|} \to 0$ as expected. Note that the instability exists only for $v_0 > c_s$ while the mode is stable (see Fig. 4.3) when $v_0 < c_s$.

Similar trends are observed in general case when both the ω_0 and ω_* are finite. These are illustrated in Figs. 4.4, 4.5 and 4.6 for the case when ω_0 and ω_* are of the same sign, corresponding to the situation of the unstable, collisionless Simon-Hoh instability. For the strongly unstable case, $v_0/c_s > 1$, the instability exist even for $\nu_{\|} = 0$ (this is the collisionless Simon-Hoh instability). In this case, the sheath dissipation (finite $\nu_{\|}$) is stabilizing: the growth rate decreases as $\nu_{\|}$ increase. With the decrease of the ratio v_0/c_s, the mode goes

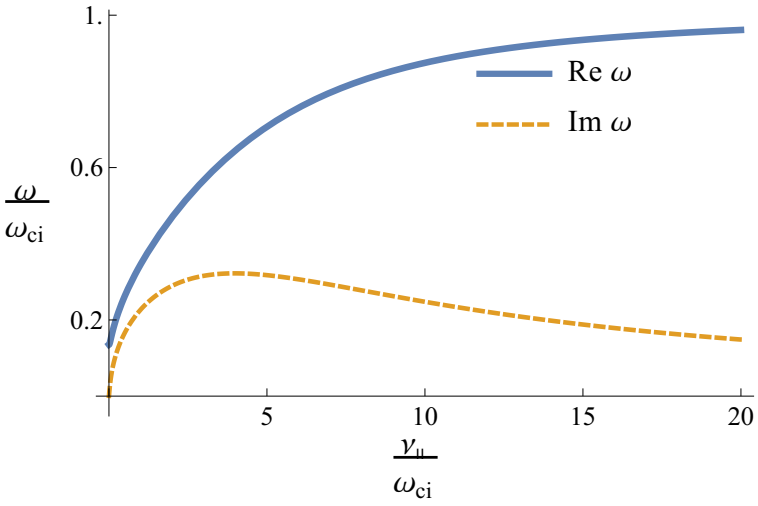

Figure 4.2: The real and imaginary part of the mode frequency as a function of $\nu_\parallel/\omega_{ci}$ for $v_0 = 0$. The maximum value of the growth rate, $\gamma \approx 0.322\omega_{ci}$, occurs at $\nu_\parallel \sim \omega_*/2$. For $\nu_\parallel \to 0$, $\omega \to k_\perp^2 c_s^2/\omega_*^2$, and for $\nu_\parallel \to \infty$, $\omega = k_y c_s$ [2].

from the weakly unstable regime to the stable regime. However as the instability drive from finite v_0/c_s is decreasing, the effect of the finite ω_* becomes more important and the mode is destabilized due to a finite $\nu_\parallel$: this is the dissipating instability of the anti-drift mode, similar the case shown in Fig. 4.2.

The collisionless Simon-Hoh instability occurs for $v_* v_0 > c_s^2/4$. This condition is not met if $v_* v_0 < 0$ or positive but too small. Then, the Simon-Hoh instability is absent, but an instability remains due to a finite $\nu_\parallel$; this situation is illustrated in Fig. 4.7. For large $\nu_\parallel$, the mode goes into the weakly unstable ions sound. In the limit of small $\nu_\parallel$, the growth rate is linearly proportional to $\nu_\parallel$ and is given by the approximate expression,

$$\gamma \approx \frac{\nu_\parallel k_y^2 c_s^2}{2\omega_*^2}\left(-1 \pm \sqrt{1 - \frac{4\omega_0\omega_*}{k_y^2 c_s^2}\left[\frac{2\omega_*(\omega_* - \omega_0)}{k_y^2 c_s^2 - 4\omega_0\omega_*} - 1\right]}\right). \tag{4.20}$$

For one of the roots (shown in Fig. 4.7), the maximum growth rate decreases with an increase of the ratio of the absolute value ω_0/ω_* when it remains negative. On the other hand, the other root has negative growth rate for the ratio $\omega_0/\omega_* > -1$ and increases with the increase of the ratio of the absolute value of ω_0/ω_* when it remains negative. For large values, the behavior of the growth rate of this root is similar to the case $\omega_* = 0$ shown in Fig. 4.3. Therefore, various regimes of dissipative instabilities of the gradient drift mode can be realized depending on typical values of plasma parameters which vary between various types

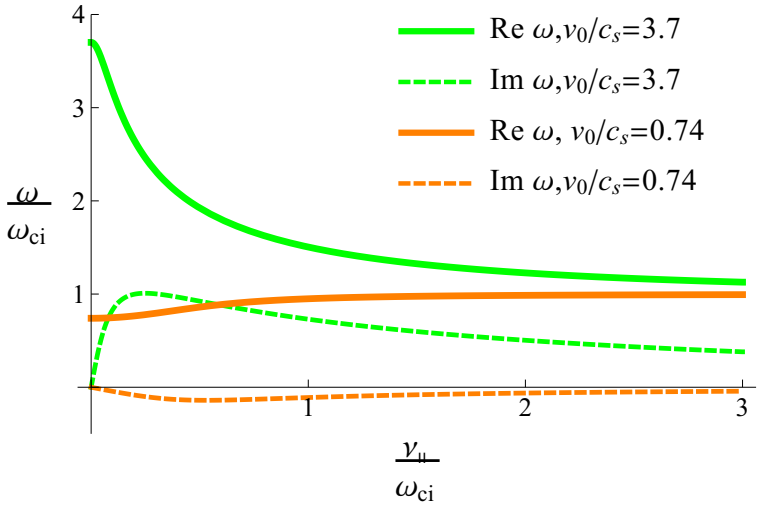

Figure 4.3: ω/ω_{ci} as a function of $\nu_{\|}/\omega_{ci}$ for $k_y\rho_s = 1$ and vanishing v_*. In the opposite limit of $\nu_{\|} \to \infty$, one finds $\omega = \omega_{ci}$ as expected. The maximum value of the growth rate, $\gamma \approx \omega_0/3$, occurs at $\nu/\omega_{ci} \approx c_s/v_0$. In the limit of vanishing $\nu_{\|} \to 0$, $\omega = \omega_0$ [2].

of $\mathbf{E} \times \mathbf{B}$ devices (e.g. Hall thruster, Penning discharge and magnetron). Plasma parameters may also vary for different regions in the same device and/or the devices of the same type (e.g. for different realizations of the Hall thrusters). For the most common types of Hall thrusters, the value of the $\mathbf{E} \times \mathbf{B}$-drift velocity v_0 may range from $10^8\ cm/s$ to vanishingly small and negative values near the anode; the plasma density gradient length scale may be in the range $L_n = 0.2 - 1\ cm$ or larger and the electron temperature T_e from a few eV to several tens of eV (see Ref [35] and references therein for a more detailed description of various Hall thruster parameters). The wide range of parameters for some $\mathbf{E} \times \mathbf{B}$ devices are given in Table 4.1. Due to the wide range of plasma parameters in various situations, one can expect that different regimes exist in the dispersion equations 4.11 and 4.17 and shown in Figs. 4.2-4.7 that may occur in different devices and different operational regimes.

4.4 Summary

In this chapter, we have investigated the role of the sheath plasma boundaries on the gradient drift instabilities in partially magnetized plasmas with $\mathbf{E} \times \mathbf{B}$ field configuration (Hall plasma). It was found that the sheath resistivity results in a dispersion equation analogous to the collisional plasma, but the resistive diffusion frequency parameter $k_z^2 v_{Te}^2/\nu_{en}$ is replaced

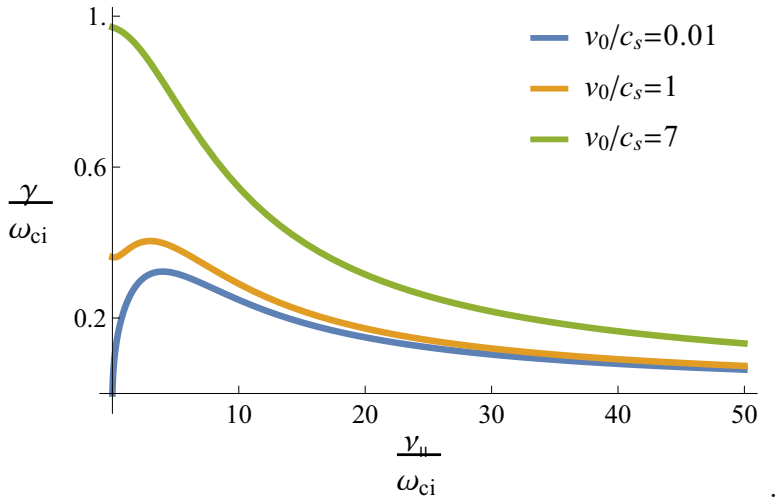

Figure 4.4: γ/ω_{ci} as a function of $\nu_{\|}/\omega_{ci}$ for $k_y\rho_s = 1$ and $\omega_*/\omega_{ci} \sim 7$. The maximum of the growth rate increases with ω_0 [2].

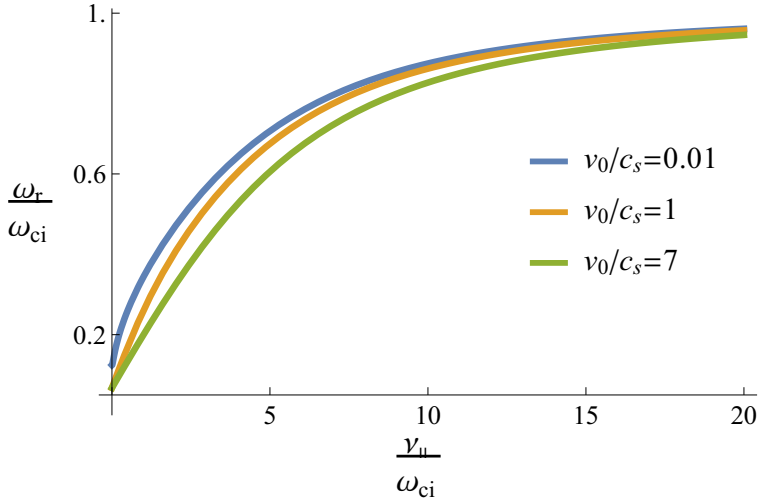

Figure 4.5: ω_r/ω_{ci} as a function of $\nu_{\|}/\omega_{ci}$ for $k_y\rho_s = 1$ [2].

with the sheath resistivity parameter c_s/L. The sheath dissipation is more important than the standard collisional resistivity when $\lambda/L > \sqrt{m_e/m_i}$. We have shown that the sheath resistivity may result in long wavelength instabilities which are driven either by the $\mathbf{E} \times \mathbf{B}$-drift or the density gradient drifts alone and in situations where the collisionless Simon-Hoh instability is not operative; this is the most important result of this chapter.

This approach was restricted to modes satisfying the condition $k_z^2 \ll k_y^2$ as well as in neglect of any kind of steady-state ion dynamics along the magnetic field. However, as seen previously, the static sheath can be maintained only when a net ion flow entering it exists.

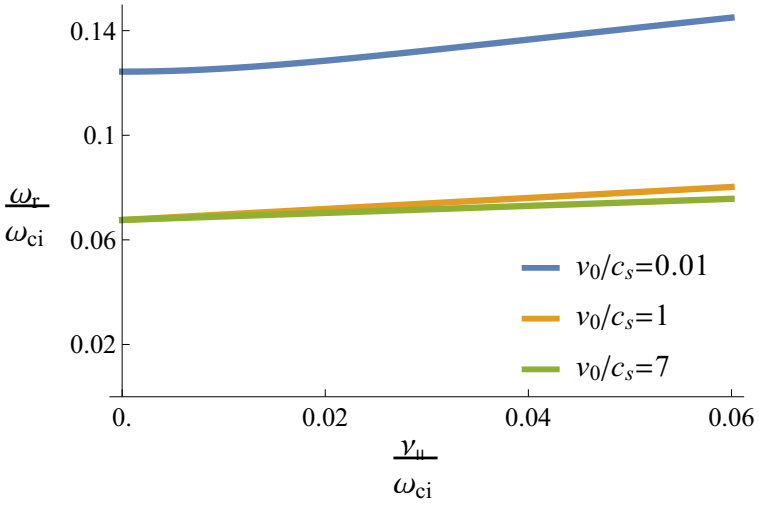

Figure 4.6: ω_r/ω_{ci} as a function of (small) $\nu_\parallel/\omega_{ci}$ for $k_y\rho_s = 1$ [2].

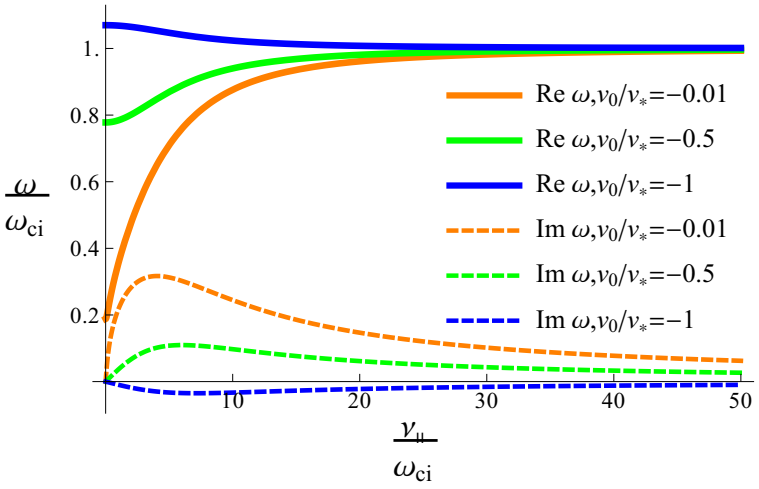

Figure 4.7: ω/ω_{ci} as a function of $\nu_\parallel/\omega_{ci}$ [2].

Therefore, the next chapter will explore the more general situation of a net ion flow along the z-axis.

Table 4.1: Penning discharge and magnetrons parameters in different regimes. The plasma length along the magnetic field in Ref [1] ($L = 0.4\,\mathrm{cm}$) is an estimate and we have estimated that $\nu_{en} \sim 10^6$ Hz for the electron-neutrals collision frequency [2].

Parameter	Ref. [36, 37]	Ref. [38]	Ref. [1]
$T_e\,(eV)$	10	5.5	3.1
Gas	Xe	Ar	Ar
$B_0\,(G)$	100	100	6000
$E_0\,(V/cm)$	1	20	116
$L_n\,(cm)$	-5	-1.2	-0.2
$L\,(cm)$	10	170	0.4
v_0/c_s	3.7	55	7.1
v_*/c_s	7.4	13	0.95
$\omega_{ci}\,(Hz)$	7.3×10^3	24×10^3	1440×10^3
$k_z^2 v_{Te}^2/\nu_{en}\omega_{ci}$	2.4×10^4	14	2.4×10^4
$c_s/L\omega_{ci}$	3.7	0.089	0.47

Chapter 5

Boundary Value Problem for a Perturbed Hall Plasma with Sheath Effects

This chapter will, for the first time, explore the stability of bounded Hall plasmas in the presence of a net ion flow along the magnetic field and satisfying the sheath boundary condition. The result is a set of two nonlinear, ordinary differential equations in the perturbed electric potential and ion velocity along the z-axis with a nonlocal integral condition. Then, the boundary conditions at the center of the plasma ($\phi(0) = \phi'(0) = 0$) will be given as well as the sheath boundary condition appropriate for this problem.

5.1 Introduction

The problem of confined, planar plasma as been extensively studied in the past [7, 16, 20, 39]. Due to the presence of dielectric walls, the electrons near the walls are removed from the plasma. In the time scale of the electron dynamics, they will accumulate on the surface of the walls leaving the region of the plasma close to the walls (to within a few Debye lengths) positively charged. The electrons in the plasma will then distribute themselves isothermally along the direction perpendicular to the walls. The positively-charged region near the walls is usually referred to as the sheath region, but there is much debate regarding the definition of the plasma-sheath boundary [19].

One may consider, at steady state, three regions of importance for the problem at hand: the plasma region where quasi-neutrality applies, the sheath region mostly devoid of electrons where Poisson's equation must be used, and the dielectric walls where there is a surface charge density due to the accumulated electrons from the sheath. The problem is essentially

a boundary-valued problem for the perturbation electric potential; the goal is to determine the stability of this perturbation when dielectric walls (and the accompanying sheath region) are present. In the plasma region, one uses quasi-neutrality with the equations of motion of the ions and electrons as well as their conservation equations. To zeroth-order, the electrons are distributed isothermally along the magnetic field lines and there is a net cross-field and diamagnetic drift. The ions, on the other hand, are assumed cold and unmagnetized; there is, however, a net drift due to the distribution of the electrons along the magnetic field lines. This net drift as well as a source of ions are necessary for mass, momentum and energy conservation throughout the plasma and sheath regions. Here, the drift velocity of the ions will be assumed to be due to the first-order term in the zeroth-order electric potential present in the plasma.

In this project, the walls will be assumed dielectric following the works of A. I. Smolyakov [21] and W. Frias [40] in which the perturbed plasma current entering the plasma sheath is equal to the displacement current in the dielectric. It is important to note that the surface charge density on the wall as well as the (approximately) isotropic ion distribution in the sheath only affect the background, constant electric potential and not the perturbed potential.

The previous chapter explored, in the approximation of $k_z^2 \ll k_y^2$, the effect of sheath on the stability of Hall plasmas. It was determined that the plasma, in the presence of sheath resistivity, behaves very much like a collisional plasma and therefore modified the Simon-Hoh instability condition (making the instability possible for values of v_0 and v_* for which the system would be stable otherwise). Further, it was shown that the sheath resistivity may result in long wavelength instabilities driven by the $\mathbf{E} \times \mathbf{B}$ electron drift or the density gradient drifts alone and in situations where the collisionless Simon-Hoh instability is not operative. To explain the full effect of the sheath on the stability of the plasma, one needs to take into account the finite size of the plasma along the magnetic field line; therefore, one needs to solve a boundary-valued problem.

The main purpose of this chapter is two-fold. First, the differential equations to be satisfied by the perturbed electric potential and ion velocity in the plasma will be derived whilst taking into account the equilibrium state of the plasma when a sheath exist (as mentioned previously, the equilibrium state defers significantly from the case where the sheath

is neglected). Second, the appropriate sheath boundary condition will be derived by considering the sheath as devoid of electrons and where the ions are distributed according to Child-Langmuir's law.

5.2 Basic Equations

Consider the z-direction to be perpendicular to the walls with the origin at the center of the plasma, the x-direction to be along the axial direction of the Hall thruster as well as $\mathbf{B} = B_0\mathbf{z}$ and $\mathbf{E}_0 = E_0\mathbf{x} + (T_e/e)(z/L^2)\mathbf{z}$. The electric field includes a constant electric field along the Hall thruster axis of symmetry (which yields the Simon-Hoh Instability) and a small electric field along the magnetic field lines which accelerates the ions to Bohm's velocity at $z = L$ necessary to satisfy Bohm's condition for a quasi-neutral plasma with plasma sheaths.

For a quasi-neutral plasma, the exact solution for the electric potential with uniform and constant ion generation rate λ is given by,

$$\frac{\lambda z}{c_s} = \frac{2\sqrt{2}}{\pi} D\left(\sqrt{\frac{e\phi}{T_e}}\right), \tag{5.1}$$

where $D(x)$ is Dawson's function [16]. This expression is, however, impractical since it cannot be inverted analytically. However, typical electron temperatures in Hall plasmas are such that $e\phi/T_e \ll 1$; this condition is violated only in the sheath region when the normalized electric potential increases drastically from the sheath potential to the wall potential. Therefore, the electric potential in the sheath region will be considered separately.

One may then approximate Dawson's function as a polynomial in its argument, keeping only the first-order term in the electric potential (the error, as it turns out, is of third-order). Then, choosing an appropriate generation rate λ, one finds the simple expression,

$$-\frac{e\phi(z)}{T_e} \approx \frac{z^2}{2L^2}. \tag{5.2}$$

Hence, at steady-state the ion drift along the magnetic field is given by,

$$\frac{\partial}{\partial z}\left(v_{i,z}^2 - c_s^2\frac{z^2}{L^2}\right) = 0. \tag{5.3}$$

It should be noted that, for the purpose of this paper, the ion drift along the x-direction will be assumed much smaller than its drift along the magnetic field and will be omitted entirely. Further, the presence of an electric field in the plasma does not imply that quasi-neutrality is lost; in fact, equation (1) was derived under the assumption of quasi-neutrality. One may verify this by using Poisson's equation,

$$-\lambda_D^2 \nabla^2 \frac{e\phi}{T_e} = \frac{\lambda_D^2}{L^2} = \left(\frac{\tilde{n}_i}{n_{i0}} - \frac{\tilde{n}_e}{n_{e0}} \right). \tag{5.4}$$

Since $\lambda_D^2 \ll L^2$, we recover quasi-neutrality everywhere in the plasma. The equilibrium number density $n_{i0} = n_{e0} = n_0(x) e^{e\phi/T_e}$ is then a function of z also.

The flux of electrons along the perpendicular directions to the magnetic field, neglecting electron inertia, is then given by,

$$\mathbf{\Gamma}_{e\perp} = \frac{v_{Te}^2}{\omega_{ce}} \left[n_e \frac{e\mathbf{E}_\perp}{T_e} + \nabla_\perp n_e \right] \times \mathbf{z}, \tag{5.5}$$

where $\mathbf{z}$ is the unit vector in the direction of the magnetic field. Along the z-axis, one finds, from the equation of motion of the electron, the condition on the electric potential and the number density,

$$\frac{\partial}{\partial z} \left(\frac{e\Phi}{T_e} - ln \left(\frac{n_e}{n_{e0}} \right) \right) = 0, \tag{5.6}$$

which, to zeroth-order, is just the Boltzmann distribution for isothermal electrons, $n_{e0} = n_0(x) e^{e\phi(z)/T_e}$. Linearizing for small perturbations in the electric potential, number density and velocity,

$$\frac{e\phi}{T_e} = -\frac{z^2}{2L^2} + \frac{e\tilde{\Phi}(z)}{T_e} e^{i(\mathbf{r}_\perp \cdot \mathbf{k}_\perp - \omega t)}, \tag{5.7}$$

$$n_e = n_{e0}(x) e^{-z^2/2L^2} + \tilde{n}_e(z) e^{i(\mathbf{r}_\perp \cdot \mathbf{k}_\perp - \omega t)}, \tag{5.8}$$

$$\mathbf{v}_e = \mathbf{v}_{0e} + \tilde{v}_e(z) e^{i(\mathbf{r}_\perp \cdot \mathbf{k}_\perp - \omega t)}, \tag{5.9}$$

one finds,

$$\tilde{\mathbf{\Gamma}}_{e\perp} = -\frac{v_{Te}^2}{\omega_{ce}} (\mathbf{z} \times i\mathbf{k}_\perp) \left[n_{e0} \frac{e\tilde{\Phi}}{T_e} - \tilde{n}_e \right] - \frac{\tilde{n}_e v_{Te}^2}{\omega_{ce}} \frac{eE_0}{T_e} \mathbf{y}, \tag{5.10}$$

and,

$$\frac{\partial}{\partial z}\left(\frac{e\tilde{\Phi}}{T_e}-\frac{\tilde{n}_e}{n_{e0}}\right)=0. \tag{5.11}$$

From the electron continuity equation, one therefore finds,

$$(\omega-\omega_0)\,\tilde{n}_e-n_{e0}\omega_*\frac{e\tilde{\Phi}}{T_e}-\frac{i}{e}\frac{d\tilde{J}_{ez}}{dz}=0, \tag{5.12}$$

where $\omega_0=-k_y(cE_0/B_0)$ and $\omega_*=k_y(cT_e/eB_0L_n)$.

The linearized equation of motion for the unmagnetized ions yields,

$$\tilde{\mathbf{v}}_{i\perp}=-\frac{ic_s^2}{\omega}\frac{e(i\mathbf{k}_\perp)\tilde{\Phi}}{T_e}, \tag{5.13}$$

$$\left(\omega+\frac{ic_s}{L}+\frac{ic_s}{L}z\frac{\partial}{\partial z}\right)\tilde{v}_{iz}=-ic_s^2\frac{e}{T_e}\frac{d\tilde{\Phi}}{dz}. \tag{5.14}$$

The continuity equation for the ions is given by,

$$\frac{\partial\tilde{n}_i}{\partial t}+\nabla\cdot(\tilde{n}_i\mathbf{v}_{i0}+n_{i0}\tilde{\mathbf{v}}_i)=-i\omega\tilde{n}_i+\frac{\partial}{\partial z}\left(\tilde{n}_iv_{i0z}+n_{i0}\tilde{v}_z\right)+\nabla_\perp\left(\tilde{n}_i\mathbf{v}_{i0\perp}+n_{i0}\tilde{\mathbf{v}}_{i\perp}\right). \tag{5.15}$$

Since we assume only a net ion flow along the z-direction, the term in $\mathbf{v}_{0\perp}$ drops. Multiplying by a factor of i, one finds,

$$\begin{aligned}&\omega\tilde{n}_i+i\frac{c_sz}{L}\frac{\partial}{\partial z}\tilde{n}_i+i\frac{c_s}{L}\tilde{n}_i+i\frac{\partial}{\partial z}\left(n_0(x)e^{-z^2/2L^2}\right)\tilde{v}_{iz}+in_0(x)e^{-z^2/2L^2}\frac{\partial}{\partial z}\tilde{v}_{iz}+i\frac{dn_0(x)}{dx}e^{-z^2/2L^2}\tilde{v}_{ix} \\ &+in_0(x)e^{-z^2/2L^2}\nabla_\perp\cdot\tilde{\mathbf{v}}_\perp=\left(\omega+i\nu_\parallel+i\nu_\parallel z\frac{\partial}{\partial z}\right)\tilde{n}_i-i\left(n_0\nu_\parallel\frac{z}{L}-n_0e^{-z^2/2L^2}c_s\frac{\partial}{\partial z}\right)\frac{\tilde{v}_{iz}}{c_s}+in_0e^{-z^2/2L^2}\frac{c_s^2k_\perp^2}{\omega}\frac{e\tilde{\Phi}}{T_e}=0.\end{aligned} \tag{5.16}$$

where $L_n^{-1}=(1/n_0)d(n_0)/dx$, $\nu_\parallel=c_s/L$ and the term in k_x/L_n was neglected. Applying the differential operator $\partial/\partial z$ to the Eq. 5.16 as well as assuming quasi-neutrality, one can combine Eqs. 5.11 and 5.16 to yield,

$$\begin{aligned}&\left(\omega+2i\nu_\parallel+i\nu_\parallel z\frac{\partial}{\partial z}\right)\frac{\partial}{\partial z}\frac{e\tilde{\Phi}}{T_e}-i\frac{\partial}{\partial z}\left(\nu_\parallel\frac{z}{L}-e^{-z^2/2L^2}c_s\frac{\partial}{\partial z}\right)\frac{\tilde{v}_{iz}}{c_s} \\ &+i\frac{c_s^2k_\perp^2}{\omega}\frac{\partial}{\partial z}\left(e^{-z^2/2L^2}\frac{e\tilde{\Phi}}{T_e}\right)=\left(\omega+2i\nu_\parallel+i\nu_\parallel z\frac{\partial}{\partial z}\right)\frac{\partial}{\partial z}\frac{e\tilde{\Phi}}{T_e} \\ &-i\frac{\partial}{\partial z}\left(\nu_\parallel\frac{z}{L}-e^{-z^2/2L^2}c_s\frac{\partial}{\partial z}\right)\frac{\tilde{v}_{iz}}{c_s}+i\frac{c_s^2k_\perp^2}{\omega}\frac{\partial}{\partial z}\left(e^{-z^2/2L^2}\frac{e\tilde{\Phi}}{T_e}\right)=0.\end{aligned} \tag{5.17}$$

Distributing the differential operator, the equation reduces to,

$$\left(\omega + 2i\nu_{\parallel} + i\nu_{\parallel} z\frac{\partial}{\partial z}\right)\frac{\partial}{\partial z}\frac{e\tilde{\Phi}}{T_e} - i\frac{\nu_{\parallel}}{L}\left(1 + z\frac{\partial}{\partial z} + e^{-z^2/2L^2}z\frac{\partial}{\partial z} - e^{-z^2/2L^2}L^2\frac{\partial^2}{\partial z^2}\right)\frac{\tilde{v}_{iz}}{c_s} + i\frac{c_s^2 k_{\perp}^2}{\omega}\left(-\frac{z}{L^2}e^{-z^2/2L^2} + \frac{\partial}{\partial z}\right)\frac{e\tilde{\Phi}}{T_e} = 0, \tag{5.18}$$

where the perturbed ion velocity along the magnetic field satisfies,

$$\left(\omega + i\nu_{\parallel} + i\nu_{\parallel} z\frac{\partial}{\partial z}\right)\frac{\tilde{v}_{iz}}{c_s} = -ic_s\frac{\partial}{\partial z}\frac{e\tilde{\Phi}}{T_e}. \tag{5.19}$$

Eqs. 5.18 and 5.19 yield a set of two nonlinear, ordinary differential equations in $e\tilde{\Phi}(z)/T_e$ and $\tilde{v}_{iz}(z)/c_s$. These must be solved simultaneously which is here possible only numerically. The boundary conditions, however, may be derived analytically.

It should be noted that since we differentiated Eq. 5.16 and used Eq. 5.11, we must add an integral condition; this is given by integrating the electron continuity equation and integrating Eq. 5.11. Then, one has,

$$\left(\frac{e\tilde{\Phi}}{T_e} - \frac{\tilde{n}_e}{n_{e0}}\right) = \text{const} \times e^{ik_y y}, \tag{5.20}$$

where we assume periodicity in the azimutal direction.

Now, when one integrates the electron continuity equation, the perturbed electron current density leaving the plasma through the sheath must be determined. Assuming the electrons are isothermal along the magnetic field lines, the electron current density inside the plasma sheath moving towards the wall must be given by,

$$\begin{aligned} j_{ez}(z) &= -e\int_0^{\infty} v_z f(z, v_z) dv_z \\ &= -\frac{en_{e0}}{\sqrt{2\pi}v_{Te}} e^{-e(\Phi(z)-\Phi_w)/T_e}\int_0^{\infty} v_z exp\left[-\frac{mv_z^2}{2T_e}\right] dv_z \\ &= -\frac{en_{e0}v_{Te}}{\sqrt{2\pi}} e^{-e(\Phi(z)-\Phi_w)/T_e}, \end{aligned} \tag{5.21}$$

where Φ_w is the wall potential. Since there is no net current into the sheath at steady-state, we have $en_0 c_s = en_0 e^{e\Phi_w/T_e} v_{Te}/\sqrt{2\pi}$. Applying the same linearization for small perturbation in the electric potential and the electron number density, one finds the boundary condition,

$$\tilde{J}_{ez}(L) = en_{e0}(x,L)c_s\left(\frac{e\tilde{\Phi}(L)}{T_e} - \frac{\tilde{n}_e(L)}{n_{e0}}\right) \equiv en_0(x,L)c_s e^{ik_y y}, \tag{5.22}$$

setting the arbitrary constant to unity. Multiplying by $1/L$ the electron continuity equation (Eq. 5.12) and integrating over the z-direction (remembering $n_{e0}(x,z) = n_0(x)\exp[-z^2/2L^2]$), one finds,

$$\frac{(\omega - \omega_0 - \omega_*)}{C_1 ic_s/L + C_2(\omega - \omega_0)}\frac{1}{L}\int_0^L e^{-z^2/2L^2}\frac{e\tilde{\Phi}(z)}{T_e}dz = 1, \tag{5.23}$$

where $C_1 = Exp[-1/2] \approx 0.606$ and $C_2 = Erf[1/\sqrt{2}]\sqrt{\pi/2} \approx 0.856$. Eq. 5.23 is the integral condition for the perturbed electric potential we need. Given a solution to our boundary-value problem, this equation provides a dispersion equation relating the angular frequency of the perturbation to its perpendicular (k_y) and parallel (k_z) wave-vectors.

For the the boundary conditions necessary to solve the problem, one may assume $\tilde{\Phi}(0) = \tilde{\Phi}'(0) = 0$ for the differential equation of the perturbed electric potential since one is free to set the origin of the electric potential and the electric field at the center of the plasma should vanish by symmetry. Additionally, since we have another differential equation to satisfy for the perturbed ion velocity, there is a relationship between the electric field and potential at the plasma-sheath edge that will be derived in the following section.

5.3 Sheath Boundary Condition

Assuming the sheath satisfies Child's law, then the electric potential and field at a given position z' in the sheath are

$$\frac{s - z'}{\lambda_D} = \frac{\sqrt{2}}{3}\left(-\frac{2e\Phi}{T_e}\right)^{3/4}, \tag{5.24}$$

$$\lambda_D\frac{d}{dz'}\left(\frac{e\Phi}{T_e}\right) = 2^{3/4}\left(-\frac{e\Phi}{T_e}\right)^{1/4}, \tag{5.25}$$

where z' is measured from the wall. Then, the perturbed electric field at any given position is (approximately) proportional to the perturbed electric field

$$\frac{\lambda_D}{2^{3/4}}\frac{d}{dz'}\left(\frac{e\tilde{\Phi}}{T_e}\right) \approx \frac{1}{4}\frac{(-e\tilde{\Phi}/T_e)}{(-e\Phi/T_e)^{3/4}}. \tag{5.26}$$

The sheath position is found by setting $z' = 0$ and is given by

$$\frac{s}{\lambda_D} = \frac{\sqrt{2}}{3}\left(-\frac{2e\Phi_w}{T_e}\right)^{3/4}, \tag{5.27}$$

$$\frac{\delta s}{\lambda_D} = 2^{1/4}\frac{(-e\tilde{\Phi}_w/T_e)}{(-e\Phi_w/T_e)^{1/4}}, \tag{5.28}$$

where $\lambda_D^{-1} = \sqrt{4\pi n_0 e^2/T_e}$ is the (inverse) debye length, Φ_w is the wall potential at steady state (which is negative relative to the plasma potential) and it is assumed that the number density at the sheath edge is the equilibrium number density n_0. Then, a small perturbation of the wall potential $\tilde{\Phi}_w$ yields a perturbation in the location of the plasma-sheath edge. Since this location is defined to be the location at which the ions reach Bohm's velocity, one requires $v_{iz}(L - \delta s) \equiv c_s$ by definition. Then,

$$\begin{aligned} v_{iz}(L-\delta s) &\equiv v_{i0}(L-\delta s) + \tilde{v}_i(L-\delta s) \\ &= v_{i0}(L) - \left.\frac{dv_{i0}}{dz}\right|_L \delta s + \tilde{v}_i(L), \end{aligned} \tag{5.29}$$

where only terms up to first-order are retained. Because $v_{i0}(z) = c_s z/L$, we find the boundary condition on the perturbed ion velocity,

$$\frac{\tilde{v}_i(L)}{c_s} = \frac{\lambda_D}{L}2^{1/4}\frac{e\tilde{\Phi}_w/T_e}{(-e\Phi_w/T_e)^{1/4}}, \tag{5.30}$$

which yields, upon using the equation of motion of the perturbed velocity in the z direction,

$$\frac{ic_s}{\omega + ic_s/L}\left.\frac{d}{dz}\frac{e\tilde{\Phi}}{T_e}\right|_L = \frac{\lambda_D}{L}2^{1/4}\frac{e\tilde{\Phi}_w/T_e}{(-e\Phi_w/T_e)^{1/4}}, \tag{5.31}$$

where the equilibrium electric potential at the wall is given by the usual expression [15],

$$-\frac{e\Phi_w}{T_e} = ln\sqrt{\frac{m_i}{2\pi m_e}}. \tag{5.32}$$

To get an expression for the perturbed wall potential as a function of the electric potential at $z = L$, one needs to use the electron dynamics.

The perturbed current density entering the sheath at all times is equal to the displacement current within the wall. The current density entering the sheath region is given by the sum of the ion and electron current densities. Since, however, the ions are assumed to enter the sheath region with a specific velocity, c_s, and because the electron and ion current densities coming from density perturbations within the plasma cancel out, the net current density entering the sheath is simply given by the electron current density from velocity perturbations,

$$\tilde{J}_z(L) = en_0(x, L)c_s\frac{e\tilde{\Phi}(L)}{T_e}. \tag{5.33}$$

In the case of a dielectric wall, a displacement current may exist within the wall due to the time-varying electric field. Then, since $\nabla \cdot (4\pi\mathbf{j} - i\omega\mathbf{D}) = 0$, one has,

$$-4\pi\tilde{J}_z(L) = i\omega[D_z(L+s+\delta) - D_z(L+s-\delta)], \tag{5.34}$$

where s is the sheath thickness as before and δ signifies an infinitesimal distance away from the wall surface into the plasma (with the negative sign) and an infinitesimal distance into the wall (for the positive sign). Assuming the wall is isotropic and homogeneous, $D_z(L+s+\delta) = \epsilon E_z(L+s+\delta)$. The electric field within the plasma sheath is found from the equation for the electric potential in the z-direction, in other words $E_z(L+s-\delta) = -d\tilde{\Phi}_w/dz$. The electric field within the wall is given by the solution to Laplace's equation for the electric potential with the boundary condition $\tilde{\Phi}(L+s+\delta) = \tilde{\Phi}(L+s-\delta) = \tilde{\Phi}_w$. Therefore,

$$\nabla^2\tilde{\Phi} = \left(\frac{\partial^2}{\partial y^2} + \frac{\partial^2}{\partial z^2}\right)e^{ik_y y}\tilde{\Phi}(z), \tag{5.35}$$

$$0 = -k_y^2\tilde{\Phi} + \frac{d^2\tilde{\Phi}}{dz^2}, \tag{5.36}$$

$$\frac{d^2\tilde{\Phi}}{dz^2} = k_y^2\tilde{\Phi}. \tag{5.37}$$

Therefore, the solution for $\tilde{\Phi}(z)$ within the wall is given by $\tilde{\Phi}(z) = \tilde{\Phi}_w(e^{-k_y z} + Ce^{k_y z})$. To satisfy the boundary condition at infinity within the wall ($\tilde{\Phi} \to 0$ as $z \to \infty$), the first term is kept (i.e. $C = 0$). Therefore, the displacement current is given by,

$$i\omega D_z(L+s+\delta) = -i\omega\epsilon \left.\frac{d\tilde{\Phi}}{dz}\right|_{z=0} = i\omega\epsilon k_y \tilde{\Phi}_w, \tag{5.38}$$

and, using the total perturbed current density we get,

$$0 = \frac{\omega_{pi}}{\lambda_D}\frac{e\tilde{\Phi}(L)}{T_e} + i\omega\epsilon k_y \frac{e\tilde{\Phi}_w}{T_e} + i\omega \frac{e}{T_e} \left.\frac{d\tilde{\Phi}}{dz}\right|_w . \tag{5.39}$$

Assuming the perturbation of the electric potential at the wall satisfies $e\tilde{\Phi}_w/T_e \ll 1$, the perturbed electric field at the wall (Eq. 5.25) reduces to (remembering that $z' = L - z$),

$$-\frac{\lambda_D}{2^{3/4}} \left.\frac{d\tilde{\Phi}}{dz}\right|_w = \frac{1}{4}\frac{e\tilde{\Phi}_w}{T_e}\left(\ln\sqrt{\frac{m_i}{2\pi m_e}}\right)^{-1/4}. \tag{5.40}$$

Therefore, combining Eqs. 5.31, 5.39 and 5.40, the boundary condition at $z = L$ becomes

$$\frac{\omega_{pi}}{\omega}\frac{e\tilde{\Phi}(L)}{T_e} = \left[2^{1/4}\epsilon k_y L\left(\ln\sqrt{\frac{m_i}{2\pi m_e}}\right)^{1/4} - \frac{1}{2\sqrt{2}}\right]\frac{\nu_\parallel}{\omega + i\nu_\parallel} L \left.\frac{d\tilde{\Phi}}{dz}\right|_L . \tag{5.41}$$

This equation yields the final boundary condition necessary to solve the boundary-value problem.

5.4 Summary

In this chapter, we have shown that it is possible to derive a set of two nonlinear, ordinary differential equations for the perturbed electric potential and ion velocity consistent with an ion flow along the magnetic field. It was found also that the electron continuity equation becomes a nonlocal integral condition on the electric potential which, given a solution to the set of differential equations, yields a dispersion equation for the nonlinear problem. Additionally, the boundary conditions at the center of the plasma were given and a boundary condition at the sheath edge was derived which provides a functional relationship between the electric potential and field at this location. Therefore, the problem is now well defined and the next step would be to solve it numerically as an analytical solution does not seem to exist.

Chapter 6

Conclusion

The main goal of this thesis was to explore the effects of plasma sheaths on the dynamics of Hall plasmas; in particular, on their effect on the Simon-Hoh instability, an important unstable mode in this type of partially magnetized plasma. It was found that, to first-order in the scale length of the system L, the sheath boundary behaves very much like a resistive term and modifies the Simon-Hoh instability in the same way that electron-neutral collisions would. Further, it was found that when the instability condition ($4v_0v_*/c_s^2 > 1$) is not satisfied, an instability still remains being driven either by the density gradient drift or $\mathbf{E} \times \mathbf{B}$ drift alone.

Then, the boundary-value problem was considered and derived for a plasma with a static sheath and net ion flow along the magnetic field. The problem reduced to a set of two nonlocal, ordinary differential equations in the perturbed electric potential and ion velocity within the bulk plasma as well as an integral equation for the electric potential which was derived from the electron continuity equation consistent with the sheath boundary condition; assuming a solution is exists, this then yields the dispersion equation for the perturbed electric potential. The boundary conditions were given at the center of the plasma, $\phi(0) = \phi'(0) = 0$, and derived at the plasma-sheath edge from the assumption of a sheath devoid of electrons and in which the ions obey Child-Langmuir's law; this latter was found to yield a relationship between the electric potential and field at the sheath edge.

The main point of this thesis is to motivate the inclusion of boundary effects on the stability of Hall plasmas in future investigations. This is because instabilities exist with significant growth rates in situations where the classical instabilities found in "infinite" plasmas, such as the Simon-Hoh instability, would otherwise be absent; this was shown in chapter 4. Since partially magnetized plasmas, as found in Hall thrusters and magnetrons, exhibit a variety of

fluctuations driven by a variety of mechanisms [21] and the exact nature of these instabilities is still unknown, one cannot neglect any possible instability mechanism. A better understanding of the effects of sheaths on the instabilities present in the bulk plasma is therefore necessary and setting the boundary-value problem with the appropriate boundary conditions, as was done in chapter 5, is the first important step in analyzing these effects thoroughly.

References

[1] T. Ito, C.V. Young, and M.A. Cappelli. Self-organization in planar magnetron microdischarge plasmas. *Applied Physics Letters*, 106(25):254104, 2015.

[2] V. Morin and A.I. Smolyakov. Modification of the simon-hoh instability by the sheath effects in partially magnetized $\mathbf{E} \times \mathbf{B}$ plasmas. *Physics of Plasmas*, 25(8):084505, 2018.

[3] M.J. Jimenez. Particle-in-cell (PIC) simulations for electron cyclotron drift instability (ECDI), August 2018.

[4] Wikimedia Commons. File:penning trap.jpg, 2013. [Online; accessed 15-August-2018].

[5] S. Chauhan. How to simulate single particle trajectory in magnetron geometry of magnetic field?, 2014. [Online; accessed 16-July-2018].

[6] J.G. Andrews and R.H. Varey. Sheath growth in a low pressure plasma. *The physics of fluids*, 14(2):339–343, 1971.

[7] S.A. Self. Exact solution of the collisionless plasmasheath equation. *The Physics of Fluids*, 6(12):1762–1768, 1963.

[8] P.M. Bellan. *Fundamentals of Plasma Physics*. Cambridge University Press, 2008.

[9] I. Langmuir. Positive ion currents from the positive column of mercury arcs. *Science*, 58:290–291, October 1923.

[10] J.E. Allen and J.G. Andrews. A note on ion rarefaction waves. *Journal of Plasma Physics*, 4(1):187194, 1970.

[11] P.D. Prewett and J.E. Allen. Ion rarefaction waves in cylindrical and spherical geometries. *Journal of Plasma Physics*, 10(3):451458, 1973.

[12] J.G. Andrews and A.J. Shrapnel. Propagation of an ion rarefaction wave from a growing sheath. *The Physics of Fluids*, 15(12):2271–2274, 1972.

[13] J.K. Chester. Effects of expanding sheaths on operation of mercury arc rectifiers. *Journal of Science and Technology*, 37(1):2, 1970.

[14] M. Murakami and K. Nishihara. Sheath dynamics induced by ion-acoustic rarefaction wave. *Physics of Fluids B: Plasma Physics*, 5(9):3441–3446, 1993.

[15] M.A. Lieberman and A.J. Lichtenberg. *Principles of plasma discharges and materials processing*. Wiley, 1994.

[16] E.R. Harrison and W.B. Thompson. The low pressure plane symmetric discharge. *Proceedings of the Physical Society*, 74(2):145, 1959.

[17] K.B. Oldham and J. Spanier. *The fractional calculus theory and applications of differentiation and integration to arbitrary order*, volume 111. Elsevier, 1974.

[18] A. Caruso and A. Cavaliere. The structure of the collisionless plasma-sheath transition. *Il Nuovo Cimento (1955-1965)*, 26(6):1389–1404, Dec 1962.

[19] K.-U. Riemann. The bohm criterion and sheath formation. *Journal of Physics D: Applied Physics*, 24(4):493, 1991.

[20] G.S. Kino and E.K. Shaw. Twodimensional lowpressure discharge theory. *The Physics of Fluids*, 9(3):587–593, 1966.

[21] A.I. Smolyakov, O. Chapurin, W. Frias, O. Koshkarov, I. Romadanov, T. Tang, M. Umansky, Y. Raitses, I.D. Kaganovich, and V.P. Lakhin. Fluid theory and simulations of instabilities, turbulent transport and coherent structures in partially-magnetized plasmas of $\mathbf{E} \times \mathbf{B}$ discharges. *Plasma Phys Contr Fusion*, 59(014041), 2017.

[22] A. Simon. Instability of a partially ionized plasma in crossed electric and magnetic fields. *The Physics of Fluids*, 6(3):382–388, 1963.

[23] A.M. Fridman. On the phenomena of the critical magnetic field and anomalous diffusion in weakly ionized plasma. In *Soviet Physics Doklady*, volume 9, page 75, 1964.

[24] W. Frias, A. I. Smolyakov, I. D. Kaganovich, and Y. Raitses. Long wavelength gradient drift instability in Hall plasma devices. I. Fluid theory. *Physics of Plasmas*, 19(7):072112, 2012.

[25] A. I. Smolyakov, W. Frias, I. D. Kaganovich, and Y. Raitses. Sheath-induced instabilities in plasmas with $E_0 \times B_0$ drift. *Physical Review Letters*, 111(11), 2013.

[26] Y. Sakawa, C. Joshi, P.K. Kaw, F.F. Chen, and V.K. Jain. Excitation of the modified simon–hoh instability in an electron beam produced plasma. *Physics of Fluids B: Plasma Physics*, 5(6):1681–1694, 1993.

[27] F F Chen. Excitation of drift instabilities in thermionic plasmas. *Journal of Nuclear Energy. Part C, Plasma Physics, Accelerators, Thermonuclear Research*, 7(4):399, 1965.

[28] F. F. Chen. Effect of sheaths on drift instabilities in thermionic plasmas. *Physics of Fluids*, 8(4):752, 1965.

[29] F. Taccogna, S. Longo, M. Capitelli, and R. Schneider. On a new mechanism inducing anomalous transport in surface-dominated magnetically confined plasma: The sheath instability. *Nuovo Cimento Della Societa Italiana Di Fisica B-Basic Topics in Physics*, 125(5-6):529–538, 2010.

[30] T. Ito and M. A. Cappelli. Electrostatic probe disruption of drift waves in magnetized microdischarges. *Applied Physics Letters*, 94(21):211501, 2009.

[31] T. Ito, C.V. Young, and M.A. Cappelli. Self-organization in planar magnetron microdischarge plasmas. *Applied Physics Letters*, 106(25):254104, 2015.

[32] W.B. Kunkel and J.U. Guillory. Interchange stabilization by incomplete line-tying. In *Proceedings of the Seventh International Conference on Phenomena in Ionized Gases, Edited by B. Popovich and D. Toscic (Gradjevinska Knjiga, Belgrade, Yugoslavia, 1966)*, volume 2. Gradjevinska Knjiga Publishing House, Belgrade, Yugoslavia, 1966.

[33] B.B. Kadomtsev. Plasma instability. In *Proceedings of the Seventh International Conference on Phenomena in Ionized Gases, Edited by B. Popovich and D. Toscic (Gradjevinska Knjiga, Belgrade, Yugoslavia, 1966)*, volume 2, page 610, 1965.

[34] A.V. Timofeev and B.N. Shvilkin. Drift-dissipative instability of an inhomogeneous plasma in a magnetic field. *Soviet Physics Uspekhi*, 19(2):149, 1976.

[35] W. Frias, A. Smolyakov, I. Kaganovich, and Y. Raitses. Long wavelength gradient drift instability in Hall plasma devices. II. Applications. *Physics of Plasmas*, 20(5):052108, 2013.

[36] I. Romadanov, A. I. Smolyakov, W Frias, O. Chapurin, and O. Koshkarov. Simon-hoh, lower-hybrid and ion-sound instabilities in partially magnetized plasmas of $\mathbf{E} \times \mathbf{B}$ discharges: Numerical studies with matlab solver. *arXiv:-1680435*, 2016.

[37] Y. Raitses, I. Kaganovich, and A.I. Smolyakov. Effects of the gas pressure on low frequency oscillations in $\mathbf{E} \times \mathbf{B}$ discharges. *IEPC*, 307, 2015.

[38] A.M. DuBois, E. Thomas, W.E. Amatucci, and G. Ganguli. Density gradient effects on transverse shear driven lower hybrid waves. *Physics of Plasmas*, 21(6), 2014.

[39] L. Tonks and I. Langmuir. A general theory of the plasma of an arc. *Phys. Rev.*, 34:876–922, Sep 1929.

[40] W. Frias, A.I. Smolyakov, I.D. Kaganovich, and Y. Raitses. Wall current closure effects on plasma and sheath fluctuations in hall thrusters. *Physics of Plasmas*, 21(6):062113, 2014.

[41] E.T. Whittaker and G.N. Watson. *A course of modern analysis*. Cambridge university press, 1996.

Appendix A

Mathematica Code

Chapter 4 is a first-order approximation to the effect of sheaths on the Simon-Hoh instability; most of the work was done analytically. Consequently, the Mathematica code was used to create plots to compare the instability growth rate with and without boundaries as well as show the growth rate and oscillation frequency due to the sheath resistance when the Simon-Hoh instability is absent.

Parameters & Constants (Penning Trap)

```
(* Xenon plasma assumed, i.e. mass/proton mass about 131 *)

light = 3*^10; charge = 4.803*^-10; mi = 131*1.6726*^-24; m = 131*16726/9.1094;
T = 10*1.6*^-12;
E0 = 1*1*^8/light;
B0 = 100;
nd = 1*^12;  nu = 1*^6;  Ln = -5;  length = 10;

Print["omegaci"]
omegaci = charge*B0/(mi*light)
omegapi = Sqrt[4*Pi*nd*charge^2/mi];
Print["debye"]
debye = Sqrt[T/(4*Pi*charge^2*nd)] (*in cm since CGS system*)

Print["cs"]
Cs = Sqrt[T/mi]
Print["rho"]
rho = Cs/(omegaci)

(*normalized to cs*)
Print["v0"]
v0 = light*E0/B0/Cs
Print["vs"]
vs = -light*T/(charge*Ln*B0)/Cs
Print["L"]
L = length/rho

(*In units of omegaci*)
vkz = 1/L^2*m*omegaci/nu
csl = 1/L

(*db and L normalized to rho_s*)

real[db_, L_] = 1 - 4*(v0*vs + 1/(db^2*L^2));
imaginary[db_, L_] = I*4/(db*L)*(vs - v0);

omegaplus[db_, L_] = 1/2*db^2/(vs*db + I/L)*(1 + Sqrt[real[db, L] + imaginary[db, L]]);
omegaminus[db_, L_] = 1/2*db^2/(vs*db + I/L)*(1 - Sqrt[real[db, L] + imaginary[db, L]]);

omegaSH[db_] = 1/2*db/vs*(1 + Sqrt[1 - 4*v0*vs]);

GammaPlot = Labeled[
    Plot[{Im[omegaplus[trial, 1/L]], Im[omegaSH[trial]]}, {trial, 0, 2},
      PlotStyle -> {Line, Dashed}, BaseStyle -> {FontWeight -> "Bold", FontSize -> 12},
```

```
    Ticks → {Table[{i, i}, {i, 0, 2, 0.5}], Table[{i, i}, {i, 0, 12, 4}]},
    PlotLegends → Placed[{"v∥/ωci=3.7", "v∥/ωci=0"}, {0.7, 0.3}]]
  , {γ/Subscript[ω, ci], Subscript[k, ⊥] Subscript[ρ, s]}, {Left, Bottom},
  LabelStyle → Directive[Large, FontFamily → "Helvetica"]]

Export["GammaPlot.eps", GammaPlot];

OmegaPlot = Labeled[
  Plot[{Re[omegaplus[trial, 1/L]], Re[omegaSH[trial]]}, {trial, 0, 2},
    PlotStyle → {Line, Dashed}, BaseStyle → {FontWeight → "Bold", FontSize → 12},
    Ticks → {Table[{i, i}, {i, 0, 2, 0.5}], Table[{i, i}, {i, 0, 0., 0.1}]},
    PlotLegends → Placed[{"v∥/ωci=3.7", "v∥/ωci=0"}, {0.7, 0.3}]]
  , {Subscript[ω, r]/Subscript[ω, ci], Subscript[k, ⊥] Subscript[ρ, s]},
  {Left, Bottom}, LabelStyle → Directive[Large, FontFamily → "Helvetica"]]

Export["OmegaPlot.eps", OmegaPlot];

HallPlot = Labeled[
  Plot[{Re[omegaplus[trial, 1/L]], Im[omegaplus[trial, L]]}, {trial, 0, 2},
    PlotStyle → {Line, Dashed}, BaseStyle → {FontWeight → "Bold", FontSize → 12},
    Ticks → {Table[{i, i}, {i, 0, 2, 0.5}], Table[{i, i}, {i, 0, 10, 2}]},
    PlotLegends → Placed[{"Real", "Imaginary"}, {0.7, 0.3}]]
  , {ω/Subscript[ω, ci], Subscript[k, ⊥] Subscript[ρ, s]}, {Left, Bottom},
  LabelStyle → Directive[Large, FontFamily → "Helvetica"]]

Export["HallPlot.eps", HallPlot];
```

Stable SH

```
Clear[v0]
db = 1;
vs
(*Sign already switch for v0 in equations, make it positive!*)
real[v_, v0_] = 1 + 4 * (v0 * vs - v^2 / db^2);
imaginary[v_, v0_] = I * 4 * v / db * (vs + v0);

omegaplus[v_, v0_] =
  1 / 2 * db^2 / (vs * db + I * v) * (1 + Sqrt[real[v, v0] + imaginary[v, v0]]);
omegaminus[v_, v0_] = 1 / 2 * db^2 / (vs * db + I * v) *
    (1 - Sqrt[real[v, v0] + imaginary[v, v0]]);

StableSHRe = Labeled[
  Plot[{Re[omegaplus[trial, vs / 100]], Re[omegaplus[trial, vs / 2]],
    Re[omegaplus[trial, vs * 2]], Re[omegaminus[trial, vs / 100]],
    Re[omegaminus[trial, vs / 2]], Re[omegaminus[trial, vs * 2]]},
   {trial, 0, 50}, PlotRange → All, PlotStyle →
    {Orange, Green, Blue, {Orange, Dashed}, {Green, Dashed}, {Blue, Dashed}},
```

```
    BaseStyle → {FontFamily → "Times New Roman", FontSize → 10},
    Ticks → {Table[{i, i}, {i, 0, 50, 10}], Table[{i, i}, {i, -0.2, 1.4, 0.2}]},
    PlotLegends → Placed[{"Re ω,v0/v*=-0.01", "Re ω,v0/v*=-0.5", "Re ω,v0/v*=-2",
       "Im ω,v0/v*=-0.01", "Im ω,v0/v*=-0.5", "Im ω,v0/v*=-2"}, {0.75, 0.6}]]
  , {ω / Subscript[ω, ci], ν∥ / Subscript[ω, ci]}, {Left, Bottom},
  LabelStyle → Directive[Large, FontFamily → "Times New Roman"]]

Export["StableSHIm.eps", StableSHRe];

StableSHIm = Labeled[
  Plot[{Im[omegaplus[trial, vs / 100]], Im[omegaplus[trial, vs / 2]],
    Im[omegaplus[trial, vs * 2]], Im[omegaminus[trial, vs / 100]],
    Im[omegaminus[trial, vs / 2]], Im[omegaminus[trial, vs * 2]]},
   {trial, 0, 50}, PlotRange → All, PlotStyle →
    {Orange, Green, Blue, {Orange, Dashed}, {Green, Dashed}, {Blue, Dashed}},
   BaseStyle → {FontFamily → "Times New Roman", FontSize → 14},
   Ticks → {Table[{i, i}, {i, 0, 50, 10}], Table[{i, i}, {i, -0.2, 1.4, 0.2}]},
   PlotLegends → Placed[{"Re ω,v0/v*=-0.01", "Re ω,v0/v*=-0.5", "Re ω,v0/v*=-2",
       "Im ω,v0/v*=-0.01", "Im ω,v0/v*=-0.5", "Im ω,v0/v*=-2"}, {0.75, 0.6}]]
  , {ω / Subscript[ω, ci], ν∥ / Subscript[ω, ci]}, {Left, Bottom},
  LabelStyle → Directive[Large, FontFamily → "Times New Roman"]]

Export["StableSHIm.eps", StableSHIm];

StableSHp = Labeled[
  Plot[{Re[omegaplus[trial, vs / 100]],
    Re[omegaplus[trial, vs / 2]], Re[omegaplus[trial, vs]],
    Im[omegaplus[trial, vs / 100]], Im[omegaplus[trial, vs / 2]],
    Im[omegaplus[trial, vs]]},  {trial, 0, 50}, PlotRange → All,
   PlotStyle → {{Orange, Thickness[0.01]}, {Green, Thickness[0.01]},
     {Blue, Thickness[0.01]}, {Orange, Dashed, Thickness[0.007]},
     {Green, Dashed, Thickness[0.007]}, {Blue, Dashed, Thickness[0.007]}},
   BaseStyle → {FontFamily → "Times New Roman", FontSize → 12},
   Ticks → {Table[{i, i}, {i, 0, 50, 10}], Table[{i, i}, {i, -0.2, 1.4, 0.2}]},
   PlotLegends → Placed[{Style["Re ω,v0/v*=-0.01", FontFamily → "Times New Roman"],
      Style["Re ω,v0/v*=-0.5", FontFamily → "Times New Roman"],
      Style["Re ω,v0/v*=-1", FontFamily → "Times New Roman"],
      Style["Im ω,v0/v*=-0.01", FontFamily → "Times New Roman"],
      Style["Im ω,v0/v*=-0.5", FontFamily → "Times New Roman"],
      Style["Im ω,v0/v*=-1", FontFamily → "Times New Roman"]}, {0.75, 0.5}]]
  , {ω / Subscript[ω, ci], ν∥ / Subscript[ω, ci]}, {Left, Bottom},
  LabelStyle → Directive[Large, FontFamily → "Times New Roman"]]

Export["StableSHp.eps", StableSHp];

StableSHn = Labeled[
  Plot[{Re[omegaminus[trial, vs / 100]],
```

```
    Re[omegaminus[trial, vs / 2]], Re[omegaminus[trial, vs]],
    Im[omegaminus[trial, vs / 100]], Im[omegaminus[trial, vs / 2]],
    Im[omegaminus[trial, vs]]},  {trial, 0, 50}, PlotStyle →
    {Orange, Green, Blue, {Orange, Dashed}, {Green, Dashed}, {Blue, Dashed}},
   BaseStyle → {FontFamily → "Times New Roman", FontSize → 10},
   Ticks → {Table[{i, i}, {i, 50, 10}], Table[{i, i}, {i, -1.4, 0.2, 0.2}]},
   PlotLegends → Placed[{"Re ω,v0/v*=-0.01", "Re ω,v0/v*=-0.5", "Re ω,v0/v*=-1",
      "Im ω,v0/v*=-0.01", "Im ω,v0/v*=-0.5", "Im ω,v0/v*=-1"}, After]]
  , {ω / Subscript[ω, ci], ν∥ / Subscript[ω, ci]}, {Left, Bottom},
  LabelStyle → Directive[Large, FontFamily → "Times New Roman"]]

Export["StableSHn.eps", StableSHn];
```

nu Dependence vanishing v0

```
Clear[v0]
db = 1;
v0 = 0;

(*nu normalized to omegaci so that ky is normalized to rho*)
real[ν_] = 1 - 4 * ν^2 / db^2;
imaginary[ν_] = I * 4 * ν / db * vs;

omegaplus[ν_] = 1 / 2 * db^2 / (vs * db + I * ν) * (1 + Sqrt[real[ν] + imaginary[ν]]);
omegaminus[ν_] = 1 / 2 * db^2 / (vs * db + I * ν) * (1 - Sqrt[real[ν] + imaginary[ν]]);

Assuming[x > 0, FindMaximum[Im[omegaplus[x]], x]]
vs / 2

LDepNu = Labeled[
  Plot[{Re[omegaplus[trial]], Im[omegaplus[trial]]}, {trial, 0.001, 20},
   PlotStyle → {{Line, Thickness[0.01]}, {Dashed, Thickness[0.007]}},
   BaseStyle → {FontFamily → "Times New Roman", FontSize → 14},
   Ticks → {Table[{i, i}, {i, 0, 20, 5}], Table[{i, i}, {i, -1, 1, 0.4}]},
   PlotLegends → Placed[{Style["Re ω", FontFamily → "Times New Roman"],
      Style["Im ω", FontFamily → "Times New Roman"]}, {0.7, 0.78}]]
  , {ω / Subscript[ω, ci], ν∥ / Subscript[ω, ci]}, {Left, Bottom},
  LabelStyle → Directive[Large, FontFamily → "Times New Roman"]]

Export["LDepNu.eps", LDepNu];
```

nu Dependence vanishing vs

```
Clear[vs, v0]
db = 1;
light * E0 / B0 / Cs
light * E0 / B0 / Cs / 5

real[v_, v0_] = 1 - 4 * v^2 / db^2;
imaginary[v_, v0_] = -I * 4 * v / db * v0;

omegaplus[v_, v0_] = 1 / 2 * db^2 / (I * v) * (1 + Sqrt[real[v, v0] + imaginary[v, v0]]);
omegaminus[v_, v0_] = 1 / 2 * db^2 / (I * v) * (1 - Sqrt[real[v, v0] + imaginary[v, v0]]);

LDepNuVs = Labeled[
  Plot[{Re[omegaminus[trial, light * E0 / B0 / Cs]] ,
    Im[omegaminus[trial, light * E0 / B0 / Cs]],
    Re[omegaminus[trial, light * E0 / B0 / Cs / 5]] ,
    Im[omegaminus[trial, light * E0 / B0 / Cs / 5]]},
   {trial, 0, 3}, PlotStyle → {{Green, Line, Thickness[0.01]},
     {Green, Dashed, Thickness[0.007]}, {Orange, Line, Thickness[0.01]},
     {Orange, Dashed, Thickness[0.007]}}, PlotRange → {All, {-0.5, 4}},
   BaseStyle → {FontFamily → "Times New Roman", FontSize → 14},
   Ticks → {Table[{i, i}, {i, 0, 3, 1}], Table[{i, i}, {i, -4, 4, 1}]},
   PlotLegends → Placed[{Style["Re ω,v0/cs=3.7", FontFamily → "Times New Roman"],
      Style["Im ω,v0/cs=3.7", FontFamily → "Times New Roman"],
      Style["Re ω, v0/cs=0.74", FontFamily → "Times New Roman"],
      Style["Im ω,v0/cs=0.74", FontFamily → "Times New Roman"]}, {0.7, 0.78}]]
  , {ω / Subscript[ω, ci], v∥ / Subscript[ω, ci]}, {Left, Bottom},
  LabelStyle → Directive[Large, FontFamily → "Times New Roman"]]

Export["LDepNuVs.eps", LDepNuVs];
```

nu Dependence for different v0

```
Clear[v0, v]

db = 1;
vs = -light * T / (charge * Ln * B0) / Cs;

real[v_, v0_] = 1 - 4 * (v0 * vs + v^2 / db^2);
imaginary[v_, v0_] = I * 4 * v / db * (vs - v0);

omegaplus[v_, v0_] =
  1 / 2 * db^2 / (vs * db + I * v) * (1 + Sqrt[real[v, v0] + imaginary[v, v0]]);
omegaminus[v_, v0_] = 1 / 2 * db^2 / (vs * db + I * v) *
    (1 - Sqrt[real[v, v0] + imaginary[v, v0]]);
omegaplus[0.0001, 1]
LDepv0Nu = Labeled[
  Plot[{Im[omegaplus[trial, 0.01]], Im[omegaplus[trial, 1]],
```

```
    Im[omegaplus[trial, 7]]}, {trial, 0, 50}, PlotRange → All, PlotStyle →
    {{Line, Thickness[0.01]}, {Line, Thickness[0.01]}, {Line, Thickness[0.01]}},
   BaseStyle → {FontFamily → "Times New Roman", FontSize → 14},
   Ticks → {Table[{i, i}, {i, 0, 50, 10}], Table[{i, i}, {i, -0.2, 1.2, 0.4}]},
   PlotLegends → Placed[{Style["v0/cs=0.01", FontFamily → "Times New Roman"],
      Style["v0/cs=1", FontFamily → "Times New Roman"],
      Style["v0/cs=7", FontFamily → "Times New Roman"]}, {0.8, 0.8}]]
  , {γ / Subscript[ω, ci], ν∥ / Subscript[ω, ci]}, {Left, Bottom},
  LabelStyle → Directive[Large, FontFamily → "Times New Roman"]]

Export["LDepv0Nu.eps", LDepv0Nu];

LDepv0NuReal = Labeled[
  Plot[{Re[omegaplus[trial, 0.01]], Re[omegaplus[trial, 1]],
    Re[omegaplus[trial, 7]]}, {trial, 0, 20}, PlotRange → All, PlotStyle →
    {{Line, Thickness[0.01]}, {Line, Thickness[0.01]}, {Line, Thickness[0.01]}},
   BaseStyle → {FontFamily → "Times New Roman", FontSize → 14},
   Ticks → {Table[{i, i}, {i, 0, 20, 5}], Table[{i, i}, {i, -0.2, 1.4, 0.4}]},
   PlotLegends → Placed[{Style["v0/cs=0.01", FontFamily → "Times New Roman"],
      Style["v0/cs=1", FontFamily → "Times New Roman"],
      Style["v0/cs=7", FontFamily → "Times New Roman"]}, {0.8, 0.5}]]
  , {Subscript[ω, r] / Subscript[ω, ci], ν∥ / Subscript[ω, ci]}, {Left, Bottom},
  LabelStyle → Directive[Large, FontFamily → "Times New Roman"]]

Export["LDepv0NuReal.eps", LDepv0NuReal];

LDepv0NuSmall = Labeled[
  Plot[
   {Re[omegaplus[trial, 0.01]], Re[omegaplus[trial, 1]], Re[omegaplus[trial, 7]]},
   {trial, 0, 0.06}, PlotRange → {All, {0, 0.15}}, PlotStyle →
    {{Line, Thickness[0.01]}, {Line, Thickness[0.01]}, {Line, Thickness[0.01]}},
   BaseStyle → {FontFamily → "Times New Roman", FontSize → 14},
   Ticks → {Table[{i, i}, {i, 0, 0.1, 0.02}], Table[{i, i}, {i, -0.02, 0.14, 0.04}]},
   PlotLegends → Placed[{Style["v0/cs=0.01", FontFamily → "Times New Roman"],
      Style["v0/cs=1", FontFamily → "Times New Roman"],
      Style["v0/cs=7", FontFamily → "Times New Roman"]}, {0.8, 0.2}]]
  , {Subscript[ω, r] / Subscript[ω, ci], ν∥ / Subscript[ω, ci]}, {Left, Bottom},
  LabelStyle → Directive[Large, FontFamily → "Times New Roman"]]

Export["LDepv0NuSmall.eps", LDepv0NuSmall];
```

Omega0 Dependence

```
Clear[v0, ν]
db = 1;

real[v0_, ν_] = 1 - 4 * (v0 * vs + ν^2 / db^2);
imaginary[v0_, ν_] = I * 4 * ν / db * (vs - v0);

omegaplus[v0_, ν_] =
  1 / 2 * db^2 / (vs * db + I * ν) * (1 + Sqrt[real[v0, ν] + imaginary[v0, ν]]);
omegaminus[v0_, ν_] = 1 / 2 * db^2 / (vs * db + I * ν) *
    (1 - Sqrt[real[v0, ν] + imaginary[v0, ν]]);

Omega0Dep = Labeled[
  Plot[{Re[omegaplus[trial, 0]], Im[omegaplus[trial, 0]],
    Re[omegaplus[trial, 0.01]], Im[omegaplus[trial, 0.01]]}, {trial, 0, 0.15},
   PlotStyle → {{Green, Line, Thickness[0.01]}, {Green, Dashed, Thickness[0.007]},
     {Orange, Line, Thickness[0.01]}, {Orange, Dashed, Thickness[0.007]}},
   BaseStyle → {FontFamily → "Times New Roman", FontSize → 12},
   Ticks → {Table[{i, i}, {i, 0, 0.15, 0.02}], Table[{i, i}, {i, 0, 0.15, 0.04}]},
   PlotLegends → Placed[{Style["Re ω", FontFamily → "Times New Roman"],
      Style["Im ω", FontFamily → "Times New Roman"],
      Style["Re ω, ν∥/ωci=0.01", FontFamily → "Times New Roman"],
      Style["Im ω, ν∥/ωci=0.01", FontFamily → "Times New Roman"]}, {0.7, 0.28}]]
  , {ω / Subscript[ω, ci], Subscript[v, 0] / Subscript[c, s]}, {Left, Bottom},
  LabelStyle → Directive[Large, FontFamily → "Times New Roman"]]

Export["Omega0Dep.eps", Omega0Dep];

Omega0Depbtrans = Labeled[
  Plot[{Re[omegaplus[trial, 5]], Im[omegaplus[trial, 5]],
    Re[omegaminus[trial, 5]], Im[omegaminus[trial, 5]]}, {trial, 0, 10},
   PlotStyle → {{Green, Line}, {Green, Dashed}, {Orange, Line}, {Orange, Dashed}},
   BaseStyle → {FontFamily → "Times New Roman", FontSize → 10},
   Ticks → {Table[{i, i}, {i, 0, 10, 2}], Table[{i, i}, {i, -1, 1, 0.5}]},
   PlotLegends → Placed[{"+ solution, Real", "+ solution, Imaginary",
      "- solution, Real", "- solution, Imaginary"}, {0.35, 0.25}]]
  , {ω / Subscript[ω, ci], Subscript[v, 0] / Subscript[c, s]}, {Left, Bottom},
  LabelStyle → Directive[Medium, FontFamily → "Times New Roman"]]

Export["Omega0Depbtrans.eps", Omega0Depbtrans];
```

Reversing Electric Field

```
Clear[v0, db]
v0 = -c * E0 / B0 / cs;

real[db_, ν_] = 1 - 4 * (v0 * vs + ν^2 / db^2);
imaginary[db_, ν_] = I * 4 * ν / db * (vs - v0);

omegaplus[db_, ν_] =
  1 / 2 * db^2 / (vs * db + I * ν) * (1 + Sqrt[real[v0, ν] + imaginary[v0, ν]]);
omegaminus[db_, ν_] = 1 / 2 * db^2 / (vs * db + I * ν) *
    (1 - Sqrt[real[v0, ν] + imaginary[v0, ν]]);

omegaSH[db_] = 1 / 2 * db / vs * (1 + Sqrt[1 - 4 * v0 * vs]);

(*PlotLabel→ "Growth Rate Comparison"*)
Reversev0 = Labeled[
  Plot[{Im[omegaminus[trial, 1 / L]], Im[omegaSH[trial]]}, {trial, 0, 2},
   PlotStyle → {Line, Dashed}, BaseStyle → {FontWeight → "Bold", FontSize → 12},
   Ticks → {Table[{i, i}, {i, 0, 2, 0.5}], Table[{i, i}, {i, 0, 0.6, 0.1}]},
   PlotLegends → Placed[{"ν∥/ω_ci=3.7", "ν∥/ωci=0"}, {0.8, 0.3}]]
  , {γ / Subscript[ω, ci], Subscript[k, ⊥] Subscript[ρ, s]}, {Left, Bottom},
  LabelStyle → Directive[Large, FontFamily → "Helvetica"]]

Subscript[E, ∥]
Subscript[E, ⊥]

Export["Reversev0.eps", Reversev0];
```

Appendix B

Detailed Calculations

B.1 Full Solution to the Dispersion Equation

The full solution to the quadratic equation

$$\frac{\omega_* + i\nu_z}{\omega - \omega_0 + i\nu_z} = \frac{k_\perp^2 c_s^2}{\omega^2}, \tag{B.1}$$

is given by,

$$\omega = \frac{k_\perp^2 c_s^2}{2(\omega_* + i\nu_z)} \left(1 \pm \sqrt{1 - 4\frac{(\omega_* + i\nu_z)(\omega_0 - i\nu_z)}{k_\perp^2 c_s^2}} \right), \tag{B.2}$$

or in dimensionless form,

$$\frac{\omega}{\omega_{ci}} = \frac{k_\perp^2 \rho_s^2}{2(\omega_*/\omega_{ci} + i\nu_z/\omega_{ci})} \left(1 \pm \sqrt{1 - 4\frac{(\omega_*/\omega_{ci} + i\nu_z/\omega_{ci})(\omega_0/\omega_{ci} - i\nu_z/\omega_{ci})}{k_\perp^2 \rho_s^2}} \right). \tag{B.3}$$

The real and imaginary parts are given exactly has,

$$\begin{aligned}
\Re[\omega] &\equiv \omega \\
&= \Re\left[\frac{k_\perp^2 c_s^2}{2(\omega_*^2 + \nu_z^2)} (\omega_* - i\nu_z) \left(1 \pm \sqrt{1 - 4\frac{(\omega_*\omega_0 + \nu_z^2)}{k_\perp^2 c_s^2} + 4i\nu_z \frac{(\omega_* - \omega_0)}{k_\perp^2 c_s^2}} \right) \right] \\
&= \Re\left[\frac{k_\perp^2 c_s^2}{2(\omega_*^2 + \nu_z^2)} (\omega_* - i\nu_z) \left(1 \pm \sqrt[4]{a^2 + b^2}\,(cos(\theta/2) + isin(\theta/2)) \right) \right] \\
&= \omega_* \frac{k_\perp^2 c_s^2}{2(\omega_*^2 + \nu_z^2)} \left(1 \pm \sqrt[4]{a^2 + b^2} cos(\theta/2) \right) \pm \nu_z \frac{k_\perp^2 c_s^2}{2(\omega_*^2 + \nu_z^2)} \left(\sqrt[4]{a^2 + b^2} sin(\theta/2) \right),
\end{aligned} \tag{B.4}$$

and, therefore,

$$\begin{aligned}
\Im[\omega] &\equiv \gamma \\
&= -\nu_z \frac{k_\perp^2 c_s^2}{2(\omega_*^2 + \nu_z^2)} \left(1 \pm \sqrt[4]{a^2 + b^2} cos(\theta/2) \right) \pm \omega_* \frac{k_\perp^2 c_s^2}{2(\omega_*^2 + \nu_z^2)} \left(\sqrt[4]{a^2 + b^2} sin(\theta/2) \right),
\end{aligned} \tag{B.5}$$

where $a = 1 - 4(\omega_*\omega_0 + \nu_z^2)/k_\perp^2 c_s^2$, $b = 4\nu_z(\omega_* - \omega_0)/k_\perp^2 c_s^2$ and $tan(\theta) = |b/a|$ $(0 \leq \theta \leq \pi/2)$; it is implicitly assumed that both $a > 0$ and $b > 0$. If a or b are negative, the following table shows the conversion to make for the angle θ. The reason for this has to do with the fact that the root function with complex argument is a multi-valued function; then, a branch cut is chosen along the negative real axis.

θ	a	b
$\rightarrow \theta$	> 0	> 0
$\rightarrow \pi - \theta$	< 0	> 0
$\rightarrow \theta - \pi$	< 0	< 0
$\rightarrow -\theta$	> 0	< 0

Table B.1: θ for the different signs of a and b

In the Simon-Hoh limit, $a < 0$ and $\nu_\parallel \rightarrow 0$. Then, regardless of the sign of b, one finds,

$$\omega = \frac{k_\perp^2 c_s^2}{2\omega_*}, \tag{B.6}$$

$$\gamma = \pm \frac{k_\perp^2 c_s^2}{2\omega_*} \sqrt{\frac{4\omega_* \omega_0}{k_\perp^2 c_s^2} - 1}. \tag{B.7}$$

If the electron drift vanishes, then $b = 4\nu_\parallel \omega_* / k_\perp^2 c_s^2 > 0$ and $a = 1 - 4\nu_\parallel^2 / k_\perp^2 c_s^2$. If, instead, we neglect ω_*, then $b = -4\nu_\parallel \omega_0 / k_\perp^2 c_s^2 < 0$ and $a = 1 - 4\nu_\parallel^2 / k_\perp^2 c_s^2$. Then, one finds,

$$\omega = \pm \frac{k_\perp^2 c_s^2}{2\nu_z} \left(\sqrt[4]{a^2 + b^2} sin(\theta/2) \right), \tag{B.8}$$

$$\gamma = -\frac{k_\perp^2 c_s^2}{2\nu_z} \left(1 \pm \sqrt[4]{a^2 + b^2} cos(\theta/2) \right), \tag{B.9}$$

where, depending on the sign of a, $\theta \rightarrow -\theta$ or $\theta \rightarrow \theta - \pi$. For small values of $\nu_\parallel$, the (positive) growth rate reduces to, using $cos(\theta/2) \approx 1 - \theta^2/8$,

$$\gamma \approx \frac{\nu_\parallel \omega_0^2}{k_\perp^2 c_s^2} - \frac{4\nu_\parallel^3 \omega_0^4}{k_\perp^6 c_s^6}. \tag{B.10}$$

The maximum occurs in the range of $\nu_\parallel / \omega_{ci} \sim c_s / v_0$.

B.2 Instability when the standard Simon-Hoh instability is not operative

If one reverses, say, the applied electric field, then the Simon-Hoh instability is not satisfied automatically. Then, in the limit of vanishing collision frequency $\nu_\parallel \rightarrow 0$, there is no instability present in the plasma. However, the presence of $\nu_\parallel$ introduces a new type of instability described by the equations B.4 and B.5 where the sign of $a \gtrless 0$ depends on the inequality $\omega_0 \omega_* \gtrless \nu_\parallel^2$ and $b > 0$ strictly. The growth rate of the two solutions have opposite behaviours; the positive solution goes from a maximum growth rate at $v_0 = 0$ to progressively smaller growth rates until it transitions to negative growth rates for $v_0 \sim v_*$ whereas the negative solution has progressively increasing growth rate, from negative values to positive values. Therefore, for large electron drift velocities (or correspondingly small v_*), the

negative solution yields an instability. Because of these opposite behaviours, there is a small interval of values for $v_0 \sim v_*$ for which both growth rates are slightly less than zero. For $\nu_\parallel \ll \omega_0 \sim \omega_* \gg k_\perp c_s$,

$$\omega \approx \frac{k_\perp^2 c_s^2}{2\omega_*}\left(1 \pm \sqrt[4]{\left(1+\frac{4v_0 v_*}{c_s^2}\right)^2 + \left(\frac{4\nu_\parallel(\omega_*+\omega_0)}{k_\perp^2 c_s^2}\right)^2}\right), \tag{B.11}$$

$$\gamma \approx -\nu_\parallel \frac{k_\perp^2 c_s^2}{2\omega_*}. \tag{B.12}$$

In the limit of small ω_* and $\nu_\parallel$, one finds,

$$\frac{-k_y^2 c_s^2}{2\nu_\parallel}\left(1 - \sqrt[4]{\left(1-\frac{4(\omega_*\omega_0+\nu_\parallel^2)}{k_y^2 c_s^2}\right)^2 + \frac{16\nu_\parallel^2\omega_0^2}{k_y^4 c_s^4}}\right). \tag{B.13}$$

B.3 Equation B.2 to 1st-Order in $\nu_\parallel$

In the limit of small $\nu_\parallel$, we may drop terms in $\nu_\parallel^2$ and make the following approximations,

$$a = 1 - \frac{4\omega_*\omega_0}{k_\perp^2 c_s^2}, \tag{B.14}$$

$$b = \frac{4\nu_\parallel(\omega_* - \omega_0)}{k_y^2 c_s^2}, \tag{B.15}$$

$$\sqrt[4]{a^2+b^2} \approx \sqrt{|a|}, \tag{B.16}$$

$$tan(\theta) = \frac{4\nu_z(\omega_*-\omega_0)}{k_\perp^2 c_s^2 - 4\omega_*\omega_0} \approx \theta, \tag{B.17}$$

$$cos(\theta/2) \approx 1, \tag{B.18}$$

$$sin(\theta/2) \approx \theta/2. \tag{B.19}$$

Then, we have the simple form,

$$\omega = \begin{cases} \frac{(k_y c_s)^2}{2\omega_*}\left(1 \pm \frac{\nu_\parallel}{\omega_*}\sqrt{\frac{4v_0 v_*}{c_s^2}-1}\right), a<0, \\ \frac{(k_y c_s)^2}{2\omega_*}\left(1 \pm \sqrt{1-\frac{4v_0 v_*}{c_s^2}}\right), a>0, \end{cases} \tag{B.20}$$

$$\gamma = \begin{cases} \pm\frac{k_y^2 c_s^2}{2\omega_*}\left(1 - \frac{\nu_\parallel}{\omega_*}\sqrt{\frac{4v_0 v_*}{c_s^2}-1}\left[1 \pm \frac{2v_*(v_*-v_0)}{4v_0 v_* - c_s^2}\right]\right), a<0, \\ -\nu_\parallel\frac{k_y^2 c_s^2}{2\omega_*^2}\left[1 \pm \sqrt{1-\frac{4v_0 v_*}{c_s^2}}\left(1+\frac{2v_*(v_*-v_0)}{4v_0 v_* - c_s^2}\right)\right], a>0. \end{cases} \tag{B.21}$$

It should be noted that in the case of reversing the electric field (i.e. not satisfying the Simon-Hoh condition for the instability), $a > 0$ strictly and one sets $v_0 \to -v_0$. From Eq.

B.21, depending on the inequality $4v_0v_* + c_s^2 \gtrless 2v_*(v_* + v_0)$, one may choose the positive or negative solution. Typically, $v_* \sim 10^7\, cm/s$, $v_0 \sim 10^6\, cm/s$ and $c_s \sim 10^3\, cm/s$; then, $4v_0v_* + c_s^2 < 2v_*(v_* + v_0)$ and one chooses the positive solution (an overall negative sign due to v_0 being negative transforms the last positive sign to a negative).

B.4 Equation B.2 to 2nd-Order in $\nu_\parallel$: Near the Simon-Hoh Transition to Instability

Near the Simon-Hoh transition from stable ion sound modes to the anti-drift instability, the value of $a \to 0$ approaches zero. Then, b^2 is not negligible; terms to second-order in the collision frequency are necessary to explain the behaviour of γ when both $\nu_\parallel$ and a are small.

$$
\begin{aligned}
a &\approx 1 - \frac{4(\omega_*\omega_0 + \nu_\parallel^2)}{k_\perp^2 c_s^2}, && \text{(B.22)}\\
\sqrt[4]{a^2 + b^2} &\approx \sqrt{|a|}\left(1 + \frac{b^2}{4a^2}\right), && \text{(B.23)}\\
tan(\theta) &= \frac{4\nu_z(\omega_* - \omega_0)}{k_\perp^2 c_s^2 - 4\omega_*\omega_0} \approx \theta, && \text{(B.24)}\\
cos(\theta/2) &\approx 1 - \frac{\theta^2}{8}, && \text{(B.25)}\\
sin(\theta/2) &\approx \theta/2. && \text{(B.26)}
\end{aligned}
$$

Then, we have with error of the order of $\nu_\parallel^3$,

$$
\begin{aligned}
\omega &= \begin{cases} \frac{(k_y c_s)^2}{2(\omega_*^2+\nu_\parallel^2)}\left(\omega_* \pm \omega_* \frac{b}{2\sqrt{a}} \pm \nu_\parallel\sqrt{a}\right), a < 0, \\ \frac{(k_y c_s)^2}{2(\omega_*^2+\nu_\parallel^2)}\left(\omega_* \pm \omega_*\sqrt{a}\left[1 + \frac{b^2}{8a^2}\right] \pm \nu_\parallel \frac{b}{2\sqrt{a}}\right), a > 0, \end{cases} && \text{(B.27)}\\
\gamma &= \begin{cases} \frac{(k_y c_s)^2}{2(\omega_*^2+\nu_\parallel^2)}\left(-\nu_\parallel \mp \nu_\parallel \frac{b}{2\sqrt{a}} \pm \omega_*\sqrt{a}\left[1 + \frac{b^2}{8a^2}\right]\right), a < 0, \\ \frac{(k_y c_s)^2}{2(\omega_*^2+\nu_\parallel^2)}\left(\omega_* \frac{b}{2\sqrt{a}} - \nu_\parallel \mp \nu_\parallel\sqrt{a}\right), a > 0. \end{cases} && \text{(B.28)}
\end{aligned}
$$

Therefore, for sufficiently small a (i.e. $4v_0v_*/c_s^2 \gtrsim 1$), a finite $\nu_\parallel$ actually increases the instability growth rate. When

B.5 Equation B.2 for Vanishing Perpendicular Wave-Number

In the limit of $k_\perp^2\rho_s^2 \ll 1$, the real and imaginary parts have the approximate forms (where the angle $tan(\theta) \approx (\omega_0 - \omega_*)/\nu_\parallel$ is a constant for small k_y),

$$
\omega = \pm\frac{1}{\nu_\parallel}\sqrt[4]{\left(\omega_*\omega_0 + \nu_\parallel^2\right)^2 + \nu_\parallel^2\left(\omega_* - \omega_0\right)^2}\, sin(\theta/2), \qquad \text{(B.29)}
$$

and

$$\gamma = \mp\frac{1}{\nu_\parallel}\sqrt[4]{\left(\omega_*\omega_0 + \nu_\parallel^2\right)^2 + \nu_\parallel^2\left(\omega_* - \omega_0\right)^2}sin(\theta/2), \tag{B.30}$$

which explains the large offset seen in the real part of the oscillation frequency from the Simon-Hoh limit ($\nu_\parallel \to 0$). If we take $v_0 \gg v_*$, then even for small k_y, we may have $\omega_0 \sim \nu_\parallel$ and $\omega \sim (\nu/\omega_{ci})cos(\pi/8)(k_\perp\rho_s)$ which explains the linear form for small perpendicular wavenumber away from zero.

B.6 Perturbed Electron Flux $\tilde{\mathbf{\Gamma}}_e$

$$m_e n_e \frac{d\mathbf{v}_e}{dt} = -en_e\left(\mathbf{E} + \frac{\mathbf{v}_e}{c}\times\mathbf{B}\right) - \nabla P - m_e n_e \nu v_{ez}\mathbf{z}. \tag{B.31}$$

Neglecting the inertia term and taking a cross-product with the magnetic field $\mathbf{B}$ for the perpendicular velocity, one finds,

$$\begin{aligned}
v_{e\parallel} &= -\frac{v_{Te}^2}{\nu}\left(\frac{eE_z}{T_e} + \frac{\partial}{\partial z}ln(n_e)\right), &\text{(B.32)}\\
0 &= -en_e\left(\mathbf{E}\times\mathbf{B} - \mathbf{B}\times\left(\frac{\mathbf{v}_e}{c}\times\mathbf{B}\right)\right) - \nabla P\times\mathbf{B}, &\text{(B.33)}\\
\mathbf{v}_{e\perp} &= \frac{c\mathbf{E}\times\mathbf{B}}{B^2} + \frac{v_{Te}^2}{\omega_{ce}}\frac{\nabla ln(n_e)\times\mathbf{B}}{B}. &\text{(B.34)}
\end{aligned}$$

Then, the electron flux is given by $\mathbf{\Gamma}_e = n_e\mathbf{v}_e$. Assuming the equilibrium number density is of the form $n_0(x,z) = n_0(x)e^{-z^2/L^2}$ and the externally applied fields are of the form $e\mathbf{E}/T_e = eE_0/T_e\mathbf{x} + z/L^2\mathbf{z}$ and $\mathbf{B} = B_0\mathbf{z}$, one finds,

$$\tilde{\mathbf{\Gamma}}_e = -\frac{n_0 v_{Te}^2}{\nu}\left(-\frac{\partial}{\partial z}\frac{e\tilde{\Phi}}{T_e} + \frac{\partial}{\partial z}\frac{\tilde{n}_e}{n_0}\right)\mathbf{z} - \tilde{n}_e\frac{v_{Te}^2}{\omega_{ce}}\left(\frac{eE_0}{T_e}\right)\mathbf{y} - \frac{n_0 v_{Te}^2}{\omega_{ce}}(\mathbf{z}\times i\mathbf{k}_\perp)\left(\frac{e\tilde{\Phi}}{T_e} + \frac{\tilde{n}_e}{n_0}\right). \tag{B.35}$$

In the limit of collisionless electrons ($\nu \to 0$), Eq. B.32 reduces to the relationship between E_z and n_e,

$$\frac{eE_z}{T_e} + \frac{\partial}{\partial z}ln(n_e) = 0 \tag{B.36}$$

Then, the electron flux reduces to,

$$\tilde{\mathbf{\Gamma}}_e = -\tilde{n}_e\frac{v_{Te}^2}{\omega_{ce}}\left(\frac{eE_0}{T_e}\right)\mathbf{y} - \frac{n_0 v_{Te}^2}{\omega_{ce}}(\mathbf{z}\times i\mathbf{k}_\perp)\left(\frac{e\tilde{\Phi}}{T_e} + \frac{\tilde{n}_e}{n_0}\right) \tag{B.37}$$

Appendix C

Mathematical Identities

C.1 Schlömilch's Transformation

Schlömilch's transformation, presented in Ref. [41], is useful when confronted with inverting an integral equation of the form,

$$f(x) = \frac{2}{\pi}\int_0^{\pi/2} \phi(x\sin\theta)d\theta. \tag{C.1}$$

In the example considered in this thesis,

$$f(x) = n_0 e^{-x^2}, \tag{C.2}$$

$$\phi(x\sin\theta) = \frac{\pi}{2\sqrt{2}c_s} g(x^2\sin^2\theta)\frac{dz}{d(x^2\sin^2\theta)}2x\sin\theta. \tag{C.3}$$

Eq. C.1 can be inverted for $-\pi \leq x \leq \pi$ given by,

$$\phi(x) = f(0) + x\int_0^{\pi/2} f'(x\sin\theta)d\theta. \tag{C.4}$$

Therefore, our problem becomes upon inversion,

$$\frac{\pi}{\sqrt{2}c_s} g(x^2)\frac{dz}{dx^2}x = n_0\left(1 + x\int_0^{\pi/2} e^{-x^2\sin^2\theta}(-2x\sin\theta)d\theta\right), \tag{C.5}$$

which reduces to Eq. 2.18 when bringing back the normalized electric potential $-\eta(z) = -e\phi(z)/T_e = x^2$ and $-\eta(\epsilon) = -e\phi(\epsilon)/T_e = x^2\sin^2\theta$.

C.2 Fractional Calculus

A brief mention of fractional calculus was made in the main body of this thesis. Since it is still an obscure area of applied mathematics, it is worth laying down its key ideas and results here.

Fractional calculus is the natural extension of calculus for the case of derivatives and integrals of fractional order. It further provides a common framework to describe both derivative and integrals, the latter being derivatives of negative integer order. One way of defining fractional derivatives is to use Cauchy's integral,

$$\frac{d^q f}{dz^q} = \frac{\Gamma(q+1)}{2\pi i}\oint \frac{f(y)dy}{(y-z)^{q+1}}, \tag{C.6}$$

where z is a complex variable and use it as a definition for non-integer q. Since q is no longer a positive integer, the pole at z becomes a branch cut; then, one chooses the contour to go from the origin to z under the branch point, then circle the pole counterclockwise once and finally comeback to the origin along the upper part of the branch cut. If $q < -1$, then we define $(y-z)^{q+1} = exp[(q+1)ln(y-z)]$ and the branch cut is along the line $z = y$.

Using the reflection property of the Gamma function, on finds, defining the angle to start from the real axis,

$$\begin{aligned}
\frac{d^q f}{dz^q} &= \frac{\Gamma(q+1)}{2\pi i}(1 - e^{-2\pi i(q+1)}) \int_0^z \frac{f(y)dy}{(y-z)^{q+1}} \\
&= \frac{-\pi csc(\pi q)}{2\pi i \Gamma(-q)} e^{-\pi i(q+1)} e^{i\pi}(e^{i\pi q} - e^{-i\pi q}) \int_0^z \frac{f(y)dy}{(y-z)^{q+1}} \\
&= \frac{-\pi (e^{i\pi q} - e^{-i\pi q})^{-1}}{\pi \Gamma(-q)} (-1)^{q+1}(-1)(e^{i\pi q} - e^{-i\pi q}) \int_0^z \frac{f(y)dy}{(y-z)^{q+1}} \\
&= \frac{1}{\Gamma(-q)} \int_0^z \frac{f(y)dy}{(z-y)^{q+1}},
\end{aligned} \tag{C.7}$$

which was originally due to Liouville and Riemann.

The main advantage of definition C.6 is clear: for any integer q, this definition reduces to the proper definitions for the derivative and integral of an analytic function. For positive integer $q > 0$, Cauchy's integral formula is recovered and the q^{th} derivative is defined for any function analytic within the contour of integration. For negative integer $q < 0$, the complex integral reduces to Eq. C.7 which is essentially q-nested integrals of the function f (this may be checked easily by differentiating $q-1$ times with respect to x to recover a single integral). Therefore, the transition from positive to negative integers as well as from integers to fractions is seamless.

One last theorem of interest is the composition rule. For any $Q > q$, one has,

$$\frac{d^Q}{dz^Q}\left(\frac{d^q f}{dz^q}\right) = \frac{d^{Q+q}}{dz^{Q+q}} f. \tag{C.8}$$

We are then free to define the half-integral and half-derivative of a function as,

$$\frac{d^{-1/2} f}{dz^{-1/2}} = \frac{1}{\Gamma(1/2)} \int_0^z \frac{f(y)dy}{(z-y)^{1/2}} = \frac{1}{\sqrt{\pi}} \int_0^z \frac{f(y)dy}{\sqrt{z-y}}, \tag{C.9}$$

$$\frac{d^{1/2} f}{dz^{1/2}} = \frac{d}{dz}\frac{d^{-1/2} f}{dz^{-1/2}} = \frac{d}{dz}\frac{1}{\sqrt{\pi}} \int_0^z \frac{f(y)dy}{\sqrt{z-y}} = \frac{1}{\sqrt{\pi}}\frac{f(0)}{\sqrt{z}} + \frac{1}{\sqrt{\pi}} \int_0^z \frac{f'(y)dy}{\sqrt{z-y}}, \tag{C.10}$$

which are useful for many physical systems such as the one considered in this research project.

As an example, one may consider the problem of "super-diffusion" or "sub-division" characterized as follows. Given any system follwoing random motion, the mean square distance traveled by any element of the system is proportional to the elapse time to a given power α. In other words,

$$\left\langle x^2 \right\rangle \sim t^\alpha, \tag{C.11}$$

where "super-diffusion" is when $\alpha > 1$ and "sub-diffusion" is for $\alpha < 1$. Clearly then, by comparison with the classical diffusion equation $\partial f/\partial t = \partial/\partial x(D\partial f/\partial x)$, one finds,

$$\frac{\partial f}{\partial t} = \frac{\partial^\alpha}{\partial x^\alpha}\left(D\frac{\partial^\alpha f}{\partial x^\alpha}\right). \tag{C.12}$$

This equation belongs to the world of fractional calculus whenever α is not an integer. If the function is a polynomial of order k, say $f = x^k$, then the fractional derivative defined above reduces to the simple form,

$$\frac{\partial^\alpha f}{\partial x^\alpha} = \frac{\Gamma(k+1)}{\Gamma(k-a+1)}x^{k-\alpha}, \tag{C.13}$$

whenever $\alpha > 0$. This can be motivated by comparing with the analogue from ordinary calculus; in other words,

$$\frac{\partial^\alpha f}{\partial x^\alpha} = \frac{k!}{(k-\alpha)!}x^{k-\alpha}, \tag{C.14}$$

which emerges from applying, α-times, the derivative operator; then, for a non-integer α, the factorials becomes Gamma functions.